Protective effects of VIP and PACAP in SARS-CoV-2 infection

Jairo R. Temerozo[1,10,*], Carolina Q. Sacramento[2,3], Natalia Fintelman-Rodrigues[2,3], Camila R. R. Pão[2], Caroline S. de Freitas[2,3], Suelen da Silva Gomes Dias[2], André C. Ferreira[2,3,4], Mayara Mattos[2,3], Vinicius Cardoso Soares[2,5], Lívia Teixeira[2], Isaclaudia G. de Azevedo-Quintanilha[2], Eugenio D. Hottz[6], Pedro Kurtz[7,8], Fernando A. Bozza[8,9], Patrícia T. Bozza[2], Thiago Moreno L. Souza[2,3], Dumith Chequer Bou-Habib[1,10,*]

[1]Laboratory on Thymus Research, Oswaldo Cruz Institute, Fiocruz, Rio de Janeiro, RJ, Brazil; [2]Laboratory of Immunopharmacology, Oswaldo Cruz Institute, Fiocruz, Rio de Janeiro, RJ, Brazil; [3]National Institute for Science and Technology on Innovation in Diseases of Neglected Populations (INCT/IDPN), Center for Technological Development in Health (CDTS), Fiocruz, Rio de Janeiro, RJ, Brazil; [4]Iguaçu University, Nova Iguaçu, RJ, Brazil; [5]Program of Immunology and Inflammation, Federal University of Rio de Janeiro, UFRJ, Rio de Janeiro, RJ, Brazil; [6]Laboratory of Immunothrombosis, Department of Biochemistry, Federal University of Juiz de Fora (UFJF), Juiz de Fora, Minas Gerais, Brazil; [7]Paulo Niemeyer State Brain Institute, Rio de Janeiro, RJ, Brazil; [8]D'Or Institute for Research and Education, Rio de Janeiro, RJ, Brazil; [9]Evandro Chagas National Institute of Infectious Diseases, Fiocruz, Rio de Janeiro, RJ, Brazil; [10]National Institute for Science and Technology on Neuroimmunomodulation, Oswaldo Cruz Institute, Fiocruz, Rio de Janeiro, RJ, Brazil.

Running Title: Neuropeptides inhibit SARS-CoV-2

Key words: SARS-CoV-2/COVID-19/VIP/PACAP

Corresponding authors: Jairo R. Temerozo and Dumith Chequer Bou-Habib

Laboratório de Pesquisas sobre o Timo, Instituto Oswaldo Cruz/Fiocruz
Av. Brasil, 4365 - Manguinhos - 21040-360.
Pav. Leonidas Deane/510
Rio de Janeiro, RJ, Brazil,
Tel. +55 21 3865-8139

E-mail: jairo.jrt@gmail.com, dumith@ioc.fiocruz.br, dumith.chequer@gmail.com

Character count: 74.279

Abstract

Infection by SARS-CoV-2 may elicit uncontrolled and damaging inflammatory response, thus it is critical to identify compounds able to inhibit virus replication and thwart the inflammatory reaction. Here, we show that the immunoregulatory neuropeptides VIP and PACAP were able to inhibit SARS-CoV-2 RNA synthesis in human monocytes and viral production in lung epithelial cells, protect the cells from virus-induced cytopathicity and reduce the production of proinflammatory mediators. Both neuropeptides prevented the SARS-CoV-2-induced activation of NF-kB and SREBP1 and SREBP2, transcriptions factors involved in proinflammatory reactions and lipid metabolism, respectively, and promoted CREB activation in infected monocytes, a transcription factor with antiapoptotic activity and also a negative regulator of NF-kB. VIP levels were elevated in plasma from patients with severe COVID-19, which correlated with the inflammatory marker CRP, viral load, and survival on those patients. Our results provide scientific evidence to further support clinical investigation of these neuropeptides against COVID-19.

Introduction

Individuals with coronavirus disease 2019 (COVID-19), caused by the severe acute respiratory syndrome coronavirus 2 (SARS-CoV-2) (1), may present asymptomatic or mild disease to severe lung inflammation and the life threatening acute respiratory distress syndrome (ARDS) (2,3), besides a variety of extrapulmonary manifestations due to multiple organ infections (4). Severe SARS-CoV-2 infection is characterized by elevated serum levels of proinflammatory mediators (hypercytokinemia, also known as cytokine storm) such as, for example,

IL-2, IL-6, TNF-α, IL-8, IL-1b, IFN-γ (2,3,5,6). The dysregulated immune response and production of cytokines and chemokines are hallmarks of SARS-CoV-2 infection and have been pointed as the main cause of the severe lung damage and unfavorable clinical progression of patients with COVID-19 (3–8). Lately, the in vivo formation of neutrophil extracellular traps (NETs) in the lungs, SARS-CoV-2-induced inflammasome activation and cell death by pyroptosis, have also been considered as risk factors in critically ill COVID-19 patients (9–14).

During the inflammatory response to human pathogenic coronaviruses (hCoVs), circulating neutrophils and monocytes migrate and infiltrate the lungs (15,16) and other organs, where they release toxic amounts of neutrophil extracellular traps (9–12) and proinflammatory cytokines, thus contributing to potentiate and perpetuate the inflammation and eventually exacerbating the tissue damage (17–19). In fact, it has been reported that SARS-CoV-2 induces neutrophils to release NETs, which are present in the plasma and lungs of critically ill COVID-19 patients, suggesting that they are central components of the exacerbated inflammatory reaction occurring in individuals with COVID-19. Previous studies showed that MERS-CoV- and SARS-CoV-infected macrophages produce high levels of pro-inflammatory cytokines and chemokines (20,21), and, more recently, that lung monocytes from severe pneumonia caused by SARS-CoV-2 are potent producers of TNF-α and IL-6, whose levels were increased in the serum of the same patients (7). Also, we and other authors have found that SARS-CoV-2 induces inflammasome activation and cell death by pyroptosis in human primary monocytes, either by experimental or natural infection, which are associated with lung inflammation and are risk factors in critically ill COVID-19 patients (13,14).

Thus, it is critical to identify agents able to prevent the infection and concurrently thwart the prototypical dysregulated inflammatory reaction and tissue lesions secondary to SARS-CoV-2 infection. In this work, we evaluated whether the neuropeptides Vasoactive Intestinal Peptide (VIP) and Pituitary Adenylate Cyclase-Activating Polypeptide (PACAP), can present protective effects in SARS-CoV-2 infection. VIP and PACAP share many biological properties through their interaction with the G protein-coupled receptors VPAC1, VPAC2 and PAC1 (22), which are systemically distributed. They have well-characterized regulatory effects on the immune system and anti-inflammatory properties, including control of cell activation and differentiation, down-regulation of inflammatory cytokines and reactive oxygen species and induction of the anti-inflammatory cytokine IL-10 (23–28). Based on their consistent anti-inflammatory activities, both neuropeptides have been considered as promising therapeutic agents for autoimmune disorders and chronic inflammatory illnesses (29–31). We report here that VIP and PACAP inhibit SARS-CoV-2 gene replication in human monocytes, viral production in lung epithelial cells, and reduced cellular production of proinflammatory mediators. We also found that VIP levels were elevated in the plasma of individuals with severe manifestations of COVID-19, which correlated with survival on critically ill patients.

Results

VIP and PACAP inhibit SARS-CoV-2 RNA synthesis in human primary monocytes, protecting them from virus-mediated cytopathic effects. Based on our previous findings showing that VIP and PACAP present antiviral effects on HIV-1 infection (32,33), and on their ability to control the inflammatory response, we initially investigated whether both neuropeptides could inhibit viral life cycle in

SARS-CoV-2-infected monocytes. Thus, human primary monocytes were treated with either VIP or PACAP, then infected with SARS-CoV-2 and the replication of viral genome was measured 24 hours later. We found that VIP significantly reduced the SARS-CoV-2 RNA synthesis, achieving up to 40% and 50% inhibition at 5 nM and 10 nM, respectively (Fig. 1A). PACAP similarly inhibited levels of viral RNA synthesis with 5 nM and 10 nM (up to 50% for both doses) (Fig. 1B). In parallel, we observed that VIP and PACAP, at 10 nM each, completely protected the monocytes from the SARS-CoV-2-mediated cytopathic effect, as measured by the LDH levels in the cell culture supernatant (Fig. 1C). These results show that both neuropeptides are similarly effective in their ability to reduce SARS-CoV-2 genome replication in monocytes and to prevent the virus-induced cell death.

Receptor contribution for the VIP and PACAP mediated inhibition of SARS-CoV-2 replication. Because VIP binds the receptors VPAC1 and VPAC2, and PACAP has high affinity for PAC1, but also binds the VPAC1 and VPAC2 (22), we analyzed the role of the individual receptors in the neuropeptide-mediated inhibition of SARS-CoV-2 RNA replication. To this end, monocytes were treated with specific agonists to VPAC1, VPAC2 and PAC1 (Ala-VIP, Bay 55 9837 and Maxadilan, respectively), and then exposed to SARS-CoV-2. We found that the sole activation of VPAC1 at 1 nM, 5 nM and 10 nM, and of VPAC2 at 1 nM, significantly reduced the SARS-CoV-2 gene replication (Fig. 1D). Of note, the optimal concentrations of the receptor agonists that significantly decreased the SARS-CoV-2 RNA synthesis were similar to those of the natural receptor ligands VIP and PACAP.

We also evaluated if the combination of VIP and PACAP could reduce the viral replication, while reducing the optimal concentration, as VIP and PACAP are reported to act synergistically or in additive fashion in the inhibition of HIV-1 replication in macrophages (32). We did not observe any increase of viral inhibition activity or reduction of optimal dose when the peptides were combined, being the 10 nM dose the optimal concentration for both peptides, combined or not (Fig. 1E).

Overall, these findings suggest that VPAC1 and VPAC2 receptors are the main contributors for the VIP- and PACAP-mediated SARS-CoV-2 inhibition in monocytes, and that the sole activation of these receptors can lead to a diminished viral inhibition similar as that induced by the own neuropeptides.

VIP and PACAP inhibit SARS-CoV-2 replication in Calu-3 cells and protect them from virus-mediated cytopathic effects. We next evaluated whether VIP and PACAP could also be able to restrict the virus production in pulmonary cells, one of the major targets of SARS-CoV-2. Thus, Calu-3 cells, a lineage of epithelial lung cells highly susceptible to this virus, were infected with SARS-CoV-2 and treated with a range of concentrations of either peptide. We found that VIP decreased the productive infection, reaching up to 50% and 40% inhibition with 1 nM and 5 nM, respectively (Fig. 2A). PACAP also diminished virus production up to 40% and 50% at concentrations equivalent to 10 nM and 50 nM (Fig. 2B). The different optimal concentrations between VIP and PACAP in their ability to control the viral productive infection in Calu-3 cells might be explained by the relative abundance of the neuropeptide receptors, since it has been shown that these cells express only VPAC1 (34). However, all three receptors are reported to be expressed in lungs, with some studies showing that VPAC1 levels are much

higher than VPAC2 (the other VIP receptor) or PAC1 (to which PACAP binds with higher affinity than to VPAC1 and VPAC2 (22,35–37)). Likewise what we found for monocytes, VIP and PACAP also protected Calu-3 cells from the SARS-CoV-2-induced cytopathogenic effects, at the same optimal viral inhibitory concentrations (1 nM and 50 nM, respectively) of each neuropeptide (Fig. 2C). Using agonists for VIP and PACAP receptors we also verified that VPAC1 is the main receptor involved the inhibition of SARS-CoV-2 in Calu-3 cells, emulating the level of inhibition achieved with VIP, while the exposure to a VPAC2 agonist resulted in a more modest inhibition (Fig. 2D). The stimulus with a PAC1 agonist had no effect on viral replication (Fig. 2D).

Given that monocytes and epithelial cells can be in close proximity in the lungs, and, thus, can interact and exchange molecules, we investigated whether conditioned medium (CM) obtained by SARS-CoV-2-infected monocytes exposed to VIP or PACAP could repress the viral production in human lung cells. While the transference of CM from uninfected monocytes, treated or nor with either neuropeptide, did not modify the virus growth, the addition of CM (at 50% vol/vol – the combination of fresh medium at this ratio did not alter the basal replication of SARS-CoV-2 in Calu-3 cells, Fig. 2E) from infected monocytes increased viral replication 33% when compared to cells maintained with the equivalent combination of fresh media (Fig. 2E). However, when infected Calu-3 cells were exposed to CM from infected monocytes treated with VIP or PACAP, we observed a reduction of 30% and 21% in SARS-CoV-2 replication in these cells (Fig. 2E). This finding raises the hypothesis that both neuropeptides, besides inhibiting the SARS-CoV-2 gene replication, induce monocyte production and release of factors endowed with antiviral activity, which may increase the resistance of neighboring

cells to SARS-CoV-2 growth. This bystander effect can reduce viral propagation, thus eventually protecting the tissues from lesions secondary to SARS-CoV-2-replication and dissemination. Future studies are needed to identify the nature of these putative soluble factors.

Influence of peptidases on VIP and PACAP inhibition of SARS-CoV-2 replication in pulmonary cells. Lung cells are known to express several peptidases (38–40), whose interaction with VIP and PACAP on the cell membrane could modulate the effects of these neuropeptides, favoring or hindering the SARS-CoV-2 replication inhibitory effect. Thus, we evaluated the inhibitory potential of VIP and PACAP in SARS-CoV-2-infected Calu-3 cells in the presence of Bestatin, an inhibitor of several aminopeptidases, including aminopeptidase N, which also acts as receptor for the human coronavirus E229 (41), but not for SARS-CoV-2 (42). While Bestatin alone (500 nM) did not change the virus yield (Fig. 3A), we verified a gain of effect of VIP at 0.5 nM and 10 nM when combined with Bestatin, (Fig. 3B). Moreover, PACAP achieved an optimal inhibitory concentration at 5 nM when combined with Bestatin, a dose ten-times lower than its optimal inhibitory concentration when alone (50 nM) (Fig. 3C). This result suggests that VIP and PACAP could be targeted by some of the peptidases expressed in pulmonary cells, thus requiring a high concentration to inhibit SARS-CoV-2 replication in these cells.

Association with antivirals increments the neuropeptide anti-SARS-CoV-2 effect in pulmonary cells. Given the enhancement of PACAP-mediated SARS-CoV-2 inhibition when in the presence of a protease inhibitor, we tested whether the association of the neuropeptides with the protease-targeting antivirals could

also increase VIP and PACAP inhibition of SARS-CoV-2 replication in pulmonary cells, as several viral protease inhibitors can also target cell proteases and peptidases (43). We tested the combination of VIP or PACAP with atazanavir, a classical HIV-1 protease inhibitor which also inhibits SARS-CoV-2 (44), or with ritonavir (whose aminopeptidase inhibition is more prominent than atazanavir (43)). For comparison, we also evaluated the combination with remdesivir, an inhibitor of RNA-dependent RNA polymerase and potent inhibitor of SARS-CoV-2 replication in vitro (45). The concentrations used for atazanavir (ATV) and ritonavir (RDV) were 5 uM, which did not significantly inhibit SARS-CoV-2 replication (Fig. 4A). The combination the neuropeptides with ATV, did not promote any increment in the inhibition of SARS-CoV-2 replication (Fig. 4B and 4C). However, when in combination with RTV, VIP and PACAP performed better than alone, with a higher inhibition with VIP+RTV at 5 nM than VIP alone at the same concentration; and PACAP achieving an optimal inhibitory concentration of 5 nM (Fig. 4C), equal to that observed when combined to Bestatin (Fig. 3C). Surprisingly, the association of VIP or PACAP with remdesivir (RDV) resulted in a strong potentiation of VIP and PACAP inhibition of SARS-CoV-2 replication in Calu-3 cells (Fig. 4B and 4C).

VIP and PACAP reduce production of proinflammatory cytokines by SARS-CoV-2-infected monocytes and Calu-3 cells. Given the hypothesis that controlling the production of proinflammatory cytokines may be critical for reducing SARS-CoV-2 replication and limiting tissue damages, and based on evidence that VIP and PACAP can regulate the inflammatory response (27,46), we next evaluated whether both neuropeptides could attenuate the production of proinflammatory mediators by SARS-CoV-2-infected monocytes or lung epithelial cells. As shown in Fig. 5A, SARS-CoV-2-infected monocytes produced large

amounts of the proinflammatory mediators IL-6, IL-8, TNF-α and MIF relative to uninfected cells (15, 4, 12 and 18 times more, respectively). In contrast, the treatment of monocytes with either neuropeptide after SARS-CoV-2 infection reduced to 66%, 50%, 66% and 50% the cellular production of IL-6, IL-8, TNF-α and MIF, respectively. Furthermore, VIP and PACAP reverted by approximately the same degree the release of IL-6 and IL-8 by Calu-3 cells (Fig. 5B), implying that VIP and PACAP may offer a critical protection to inflamed lungs affected by SARS-CoV-2 replication. Because proinflammatory cytokines may favor SARS-CoV-2 replication, which, in turn, can amplify the cellular synthesis of these mediators, these findings may support our assumption that VIP and PACAP offer tissue protection by inhibiting virus replication and regulating the boost of cytokine production.

VIP and PACAP regulate the activation of transcription factors in SARS-CoV-2-infected monocytes. Based on the fact that the transcription factor NF-kB is critically involved in the cellular production of inflammatory mediators (47), and on our own findings that VIP and PACAP can inhibit its activation in HIV-1-infected macrophages (33), we investigated whether both neuropeptides would exert this same effect on SARS-CoV-2-infected monocytes. As can be seen in Fig. 6A, we initially observed that NF-kB is up-modulated in infected cells (as measured by the increased amount of phosphorylated NF-kBp65 subunit) and, in addition, that VIP and PACAP reduced the NF-KBp65 phosphorylation, evidencing the significant anti-NF-kBp65 activity of VIP and PACAP. We believe that the SARS-CoV-2-induced NF-kB activation could have contributed for the elevated production of proinflammatory cytokines by SARS-CoV-2-infected monocytes, and that the inhibition of this transcription factor by VIP and PACAP was critical for the

decreased synthesis of these mediators by the same cells. Following, we analyzed the effects of both neuropeptides on the activation of CREB, a transcription factor induced by several GPCR ligands, including VIP and PACAP (48), and also involved in the induction of anti-inflammatory cytokines (49,50). CREB and NF-kB share the CREB-binding protein/p300 (CBP/p300 protein) as a cofactor, and CREB activation results in the inhibition of NF-kB (51). We found that activation of CREB was diminished in SARS-CoV-2-infected monocytes, a finding coherent with NF-kB activation in the same cells (Fig. 6B). Consistent with this finding, VIP and PACAP promoted CREB activation (as measured by augmentation of CREB phosphorylation) in those infected monocytes, a result matching the inhibition of NF-kB and the reduction of cellular production of proinflammatory cytokines.

We also evaluated in SARS-CoV-2-infected monocytes the expression of the active form of SREBP-1 and SREBP-2, a transcription factor that also interacts with CBP/p300 (52), and is crucial for the replication of several viruses, including coronaviruses (53–55). In fact, we and other authors reported that SARS-CoV-2 infection promotes the activation of SREBP, and that this activation is associated with enhanced viral replication (56) and COVID-19 disease severity(57). We found that the levels of both isoforms of SREBP in active state are increased in SARS-CoV-2-infected monocytes, but reduced in infected monocytes exposed to VIP and PACAP when compared to the untreated infected cells, lowering to the same basal levels found in uninfected monocytes (Fig. 6C and 6D, Supp. Fig. 1).

Together, these results suggest that the restriction of SARS-CoV-2 replication in monocytes and, possibly, in pulmonary cells (represented in this work by the Calu-3 cell line) by VIP and PACAP can also be the outcome of the intrinsic modulation of transcription factors related to the regulation of inflammatory

factors that are involved directly and indirectly with the viral replication, either by favoring the cellular damage, through exacerbating the inflammation, or by promoting a permissive cellular microenvironment for viral replication.

Plasma levels of VIP are elevated in patients with severe forms of COVID-19. Based on our results showing that VIP and PACAP, besides inhibiting viral replication and production, can also control the production of proinflammatory mediators by SARS-CoV-2-infected monocytes and lung epithelial cells, we measured the levels of both neuropeptides in plasma samples of SARS-CoV-2-infected individuals. We found that the amount of VIP is significantly elevated in patients affected by the most severe forms of infection, relative to levels of uninfected healthy controls and asymptomatic/mild patients (Fig. 7A). We also observed that some critically ill patients had increased levels of PACAP, but without statistical significance when considering the entire group (Fig. 7B). In addition, levels of VIP positively correlated with levels of C-reactive protein (CRP) (Fig. 7C), but neither VIP nor PACAP levels correlated with other inflammatory markers, such as D-dimer, fibrinogen or IL-6 (data not shown), or with each other (Fig. 7D). We found a positive correlation between VIP levels and viral load in positive swab samples from mild and severe COVID-19 patients (Fig. 7E and 7F). Severe COVID-19 patients admitted to the ICU were further stratified between those requiring invasive mechanical ventilation or noninvasive O_2 supplementation, or according to the 28-day mortality outcome as survivors or non-survivors. For PACAP we did not observe statistical significance in the stratified groups (Fig. 7G and 7H), the same for VIP considering respiratory support (Fig. 7I). However, we found that VIP plasma levels were significantly higher in survivors than in non-survivors (Fig. 7J).

Taking into account that VIP and PACAP regulate inflammatory reactions, it is possible that their increased circulating amounts reflect a counter-regulatory effect elicited by the dysregulated immune response typical of the more severe clinical status of COVID-19 patients. The levels of VIP and PACAP in SARS-CoV-2-infected tissues should be a matter of future studies, to support our hypothesis.

Discussion

In this work, we report that the neuropeptides VIP and PACAP, endogenous molecules presenting anti-inflammatory properties, are able to inhibit SARS-CoV-2 RNA synthesis and viral production and reduce the exacerbated synthesis of proinflammatory mediators due to infection, in human monocytes and lung epithelial cells. Also, we identified that VIP plasma levels are elevated in patients with severe forms of COVID-19, corresponding with viral load, and elevated VIP levels at ICU admission predicts patients' favorable outcome, including association with patient survival. Our findings provide the scientific basis for clinical trials with VIP (Aviptadil), which can be used in intravenous (58) and inhaled (59) formulations. Indeed, first results of clinical studies with VIP are expected to be disclosed in the next year (58,59). Clinical data, along with mechanism described here, may allow additional larger trials with VIP, an overlooked molecule associated with antiviral, anti-inflammatory and enhanced survival activities.

Both neuropeptides regulate the inflammatory response due to their ability to decrease the production of proinflammatory mediators, and to elicit the production of anti-inflammatory molecules, Given that VIP and PACAP and their receptors are systemically distributed, including the lungs (22,60), brain and gut, we believe that the anti-SARS-CoV-2 effects of both neuropeptides would not be

restricted to the respiratory tract, as shown by many studies in other chronic inflammatory illnesses.

Here, we initially observed that VIP and PACAP decreased the genome replication of SARS-CoV-2 in monocytes, in parallel with protecting the cells from virus-induced cytopathicity. By diminishing the intracellular levels of viral RNA and other viral molecules, VIP and PACAP could prevent the cell death by pyroptosis, which has been described as one of the main causes of cell damage during SARS-CoV-2 infection (13,14). While preserving the viability of monocytes, VIP and PACAP also diminished the production of the proinflammatory cytokines IL-6, IL-8, TNF-α and MIF by these cells, which is in agreement with the reported ability of these neuropeptides to regulate the inflammatory response (24–27,61). We found similar results with lung epithelial cells, further supporting the assumption that VIP and PACAP may offer a critical protection to inflamed lungs affected by SARS-CoV-2 replication. Because these mediators are elevated in patients with COVID-19, it is possible that the higher amounts of VIP in patients with severe forms of infection may reflect a counter-regulatory feedback elicited by the dysregulated immune response of these patients. Interestingly, the cellular protection conferred by VIP or PACAP to SARS-CoV-2-infected monocytes can be transferred to other neighboring virus target cells (Fig. 2E), suggesting that a bystander effect can ultimately protect other SARS-CoV-2-infected cells not directly interacting with VIP or PACAP. More investigations are needed to identify the nature of the putative protecting factors present in the monocyte supernatants.

The ability of VIP and PACAP to inhibit the SARS-CoV-2-induced activation of the subunit p65 of the transcription factor NF-kB, pertain to a complex molecular

mechanism leading to reduction of proinflammatory cytokines synthesis by SARS-CoV-2-infected monocytes. Also, we detected here that the transcription factor CREB, which can act as a negative regulator of NF-kB (62,63), is down-regulated in SARS-CoV-2-infected monocytes, in opposition to NF-kB activation in the same cells. In some models (64–69), CREB activation is related to induction of anti-inflammatory cytokines concomitant with reduction of pro-inflammatory molecules, mainly through direct transcription of its targets, such as IL-10, or through competing with NF-kB by their shared co-activator protein CBP/p300 (49,62,63,69). Besides its role in the balance between pro- and anti-inflammatory cytokines, CREB activation is also involved with the anti-apoptotic response in monocytes and macrophages, during differentiation and inflammatory stimuli (70,71). Thus, the imbalance between CREB and NF-kB, either as a direct effect of infection by SARS-CoV-2 or a consequence of exposure of bystander cells to viral products and inflammatory molecules, could be an important target for inhibition of SARS-CoV-2 deleterious effects, at least in monocytes and probably also in lung cells, as a similar imbalance between CREB and NF-kB was observed in an acute inflammatory pulmonary condition (51).

The induction of SREBP activity by SARS-CoV-2 was consistent with data showing its increase and association with COVID-19 severity in patients (57). SREBPs are transcription factors that have well-defined roles in the regulation of cellular lipid homeostasis (72). They exist in an inactive form associated to the endoplasmatic reticulum, where initial activation occurs, completing the activation in the Golgi apparatus before migrating to the nucleus (72). SREBP1 regulates the expression of fatty acid biosynthesis genes, whilst SREBP2 regulates genes involved in cholesterol biosynthesis, intracellular lipid movement and lipoprotein

import (72). While crucial for metabolic homeostasis, both transcription factors are involved in pathologies when misbalanced or overactivated (72), and several viruses are reported to induce their activation, as for their optimal replication, the up-regulation of host lipid biosynthesis is a requirement (53–55). In fact, our group just reported that SARS-CoV-2 activates SREBP-1 and other pathways of lipid metabolism in human cells, and that lipid droplets enhance viral replication and production of inflammatory mediators (56). The inhibition of SREBP activation in SARS-CoV-2-infected monocytes exposed to VIP and PACAP points to a possible mechanism of viral inhibition directly related to the replicative cycle, since inhibiting SREBPs activation, the replication process can be restrained via limiting the supply of energy and building blocks, ultimately delaying or even stopping the replicative process.

Similar to NF-kB and CREB, the association of SREBP with CBP/p300 (52) makes its function susceptible to the availability of this co-factor, which abundance can be low or high depending on the state of activation of NF-kB and CREB. Thus, the modulation of each one of these factors by VIP and PACAP can reflect a fine tuning of the transcriptional regulation of metabolic and inflammatory pathways, which in turn can affect the replication of SARS-CoV-2.

Because VIP and PACAP signaling pathway outcome is dependent of the combined action of the receptors activated by them (VIP and PACAP receptors can elicit cell signaling in homo and hetero dimers (73)), we evaluated whether they were involved in the final outcome analyzed. Our assays suggest that signaling through the receptors VPAC1 and VPAC2 contributed for VIP- and PACAP-mediated reduction of SARS-CoV-2 RNA synthesis in monocytes and viral

production in Calu-3 cells, with VPAC1 activation alone being able to reproduce the SARS-CoV-2 inhibition promoted by the natural neuropeptides. The inhibition profile of SARS-CoV-2 by VIP and PACAP in Calu-3 cells may be biased regarding the expected action in the lungs, since Calu-3 cells appear to express only VPAC1 (34). However, lung tissues, while reported to express high levels of VPAC1, also express VPAC2 and PAC1 (35,37), and, more specifically, VPAC2 mRNA was detected in airway epithelial, glandular, and immune cells of the lung (36). Therefore, while the inhibition curve of SARS-CoV-2 by VIP and PACAP in Calu-3 cells points to different optimal doses than those obtained for monocytes, it is possible that in normal lung cells and tissue, VIP and PACAP could present a broader range of action in the inhibition of SARS-CoV-2. In fact, VIP and specific agonists for VPAC1 or VPAC2 have been proposed and tested for respiratory conditions, like asthma (74–76), pulmonary arterial hypertension (PAH) (74,77,78) and chronic obstructive pulmonary disease (COPD) (74,75,79), demonstrating that the anti-inflammatory actions of VIP/PACAP can be achieved in lung tissues. Future studies should define which of these receptors would preferentially be activated by specific agonists to restrain SARS-CoV-2 replication in lungs or other sites. Together with the possible differences of receptor expression and self-regulatory characteristics of GPCRs, a third regulation level of VIP and PACAP action on pulmonary cells can be achieved by the activity of proteases and peptidases, as lungs are described to express high levels of several of them in both normal and pathological conditions (38–40). Some of these peptidases could target VIP and PACAP, thus altering the ligand/receptor ratio and modulating the signaling pathways.

The improvement of VIP and PACAP action on SARS-CoV-2 inhibition in Calu-3 cells when combined with Bestatin, suggests that some aminopeptidases are involved in the processing or degradation of these neuropeptides. Likewise, the finding that the anti-SARS-CoV-2 effect of both neuropeptides is enhanced when they were combined with RTV, which *per se* did not inhibit SARS-CoV-2 replication but can inhibit cellular peptidases (43), supports the view that a possible clinical use of VIP or PACAP for COVID-19 treatment would be aided by a concomitant inhibition of aminopeptidases. In fact, Bestatin (Ubenimex) has already been evaluated for clinical use for some types of cancer and cardiovascular diseases, with no significant side effects (80,81). The strong inhibition of virus production resulting from the combination of VIP and PACAP with remdesivir raises the possibility that the direct inhibition of SARS-CoV-2 transcription by this antiviral could alleviate the excessive metabolic burden on cellular processes, due to sheer reduction of viral load in the infected cells, ultimately favoring the antiviral and anti-inflammatory actions of VIP and PACAP on these cells.

Since up to now there are no antivirals specific to SARS-CoV-2, and that the hyper-inflammation may persist even after the lowering of the viral load, the searching for compounds that target the aberrant production of proinflammatory cytokines and, simultaneously, the own viral replication, should be stimulated. Our present results showing that VIP and PACAP hold these two critical activities point these neuropeptides or their analogue molecules as potential therapeutic agents for COVID-19.

Materials and Methods

Cells, virus and reagents. African green monkey kidney cells (Vero, subtype E6) and human lung epithelial cell lines (Calu-3) were expanded in high glucose DMEM (Vero) or MEM (Calu-3) with 10% fetal bovine serum (FBS; HyClone), with 100 U/mL penicillin and 100 µg/mL streptomycin (Pen/Strep; Gibco) at 37°C in a humidified atmosphere with 5% CO_2.

Peripheral blood mononuclear cells (PBMCs) were isolated by density gradient centrifugation (Ficoll-Paque, GE Healthcare) from buffy-coat preparations of blood from healthy donors. PBMCs (2 x 10^6 cells) were plated onto 48-well plates (NalgeNunc) in RPMI-1640 with 5% inactivated male human AB serum (Merck) for 3 hours. Non-adherent cells were removed and the remaining monocytes were maintained in DMEM (low-glucose) with 5% human serum (Merck) and 100 U/mL penicillin and 100 µg/mL streptomycin (Pen/Strep; Gibco). The purity of human monocytes was above 90%, as determined by flow cytometric analysis (FACScan; Becton Dickinson) using anti-CD3 (BD Biosciences) and anti-CD14 (BD Biosciences) monoclonal antibodies.

SARS-CoV-2 was expanded in Vero E6 cells from an isolate contained on a nasopharyngeal swab obtained from a confirmed case in Rio de Janeiro, Brazil (GenBank accession no. MT710714). Viral isolation was performed after a single passage in a cell culture in a 150 cm^2 flasks with high glucose DMEM plus 2% FBS. Observations for cytopathic effects were performed daily and peaked 4 to 5 days after infection. All procedures related to virus culture were handled in biosafety level 3 (BSL3) multiuser facilities according to WHO guidelines. Virus

titers were determined as plaque forming units (PFU/mL), and virus stocks were kept in -80°C ultralow freezers.

The neuropeptides VIP and PACAP and the VPAC1 and VPAC2 agonists ($Ala^{11,22,28}$)-VIP and Bay 55-9837, respectively, were purchased from Tocris. The PAC1 agonist Maxadilan was kindly donated by Dr. Ethan A. Lerner (Department of Dermatology, Massachusetts General Hospital, MA, USA). All peptides and agonists were diluted in PBS. The antivirals atazanavir (ATV), ritonavir (RTV) and remdesivir (RDV) were purchased from Selleckhem, dissolved in 100% dimethylsulfoxide (DMSO) and subsequently diluted at least 10^4-fold in culture or reaction medium before each assay. The final DMSO concentrations showed no cytotoxicity.

Infections and virus titration. Infections were performed with SARS-CoV-2 at MOI of 0.01 (monocytes) or 0.1 (Calu-3) in low (monocytes) or high (Calu-3) glucose DMEM without serum. After 1 hour, cells were washed and incubated with complete medium with treatments or not. For virus titration, monolayers of Vero E6 cells (2×10^4 cell/well) in 96-well plates were infected with serial dilutions of supernatants containing SARS-CoV-2 for 1 hour at 37°C. Semi-solid high glucose DMEM medium containing 2% FSB and 2.4% carboxymethylcellulose was added and cultures were incubated for 3 days at 37 °C. Then, the cells were fixed with 10% formalin for 2 hour at room temperature. The cell monolayer was stained with 0.04% solution of crystal violet in 20% ethanol for 1 hour. Plaque numbers were scored in at least 3 replicates per dilution by independent readers blinded to the experimental group and the virus titers were determined by plaque-forming units (PFU) per milliliter.

Molecular detection of virus RNA levels. The total RNA was extracted from cultures using QIAamp Viral RNA (Qiagen®), according to manufacturer's instructions. Quantitative RT-PCR was performed using QuantiTect Probe RT-PCR Kit (Quiagen®) in a StepOnePlus™ Real-Time PCR System (Thermo Fisher Scientific). Amplifications were carried out in 15 µL reaction mixtures containing 2× reaction mix buffer, 50 µM of each primer, 10 µM of probe, and 5 µL of RNA template. Primers, probes, and cycling conditions recommended by the Centers for Disease Control and Prevention (CDC) protocol were used to detect the SARS-CoV-2 (82). The standard curve method was employed for virus quantification. For reference to the cell amounts used, the housekeeping gene RNAse P was amplified. The Ct values for this target were compared to those obtained to different cell amounts, 10^7 to 10^2, for calibration.

SDS-PAGE and Western blot for SREBPs. After 24h of SARS-CoV-2 infection, monocytes were harvested using ice-cold lysis buffer (1% Triton X-100, 2% SDS, 150 mM NaCl, 10 mM HEPES, 2 mM EDTA containing protease inhibitor cocktail - Roche). Cell lysates were heated at 100 °C for 5 min in the presence of Laemmli buffer (20% β-mercaptoethanol; 370 mM Tris base; 160 µM bromophenol blue; 6% glycerol; 16% SDS; pH 6.8), and 20 µg of protein/sample were resolved by electrophoresis on SDS-containing 10% polyacrylamide gel (SDS-PAGE). After electrophoresis, the separated proteins were transferred to nitrocellulose membranes and incubated in blocking buffer (5% nonfat milk, 50 mM Tris-HCl, 150 mM NaCl, and 0.1% Tween 20). Membranes were probed overnight with the following antibodies: anti-SREBP-1 (Proteintech #14088-1-AP), anti-SREBP-2 (Proteintech #28212-1-AP) and anti-β-actin (Sigma, #A1978). After the washing steps, they were incubated with IRDye - LICOR or HRP-conjugated secondary

antibodies. All antibodies were diluted in blocking buffer. The detections were performed by Supersignal Chemiluminescence (GE Healthcare) or by fluorescence imaging using the Odyssey system. The densitometries were analyzed using the Image Studio Lite Ver 5.2 software.

Measurements of inflammatory mediators, cell death, NF-kBp65, CREB and neuropeptides. The levels of IL-6, IL-8, TNF-α and MIF were quantified in the supernatants from uninfected and SARS-CoV-2-infected Calu-3 cells and monocytes by ELISA (R&D Systems), following manufacturer's instructions, and results are expressed as percentages relative to uninfected cells. Cell death was determined according to the activity of lactate dehydrogenase (LDH) in the culture supernatants using a CytoTox® Kit (Promega, USA) according to the manufacturer's instructions. Results are expressed as percentages of released LDH compared to control cells lysed with 0.8% Triton X-100. Supernatants were centrifuged at 5,000 rpm for 1 minute, to remove cellular debris. Evaluation of NF-kBp65 and CREB activation was performed in infected or uninfected monocytes using NFkB p65 (Total/Phospho) InstantOne™ and CREB (Total/Phospho) Multispecies InstantOne™ ELISA Kits (Thermo Fisher), according to manufacturer's instructions. VIP and PACAP levels were quantified in the plasma from patients or control volunteers using standard commercially available ELISA and EIA Kits, according to the manufacturer's instructions (Abelisa).

Human subjects. We prospectively enrolled severe or mild/asymptomatic COVID-19 RT-PCR-confirmed cases, and SARS-CoV-2-negative controls. Blood and respiratory samples were obtained from the 24 patients with severe COVID-19 within 72 hours from intensive care unit (ICU) admission in two reference centers

(Instituto Estadual do Cérebro Paulo Niemeyer and Hospital Copa Star, Rio de Janeiro, Brazil). Severe COVID-19 was defined as those critically ill patients presenting viral pneumonia on computed tomography scan and requiring oxygen supplementation through either a nonrebreather mask or mechanical ventilation. Four outpatients presenting mild self-limiting COVID-19 syndrome, and two SARS-CoV-2-positive asymptomatic subjects were also included. All patients had SARS-CoV-2 confirmed diagnostic through RT-PCR of nasal swab or tracheal aspirates. Peripheral vein blood was also collected from 10 SARS-CoV-2-negative healthy participants as tested by RT-PCR on the day of blood sampling. The characteristics of severe (n=24), mild/asymptomatic (n=6) and healthy (n=10) participants are presented in **Table 1**. Mild and severe COVID-19 patients presented differences regarding the age and the presence of comorbidities as obesity, cardiovascular diseases and diabetes (**Table 1**), which is consistent with previously reported patient cohorts (2,83–85). The SARS-CoV-2-negative control group, however, included subjects of older age and chronic non-communicable diseases, so it is matched with mild and critical COVID-19 patients, except for hypertension (**Table 1**). All ICU-admitted patients received usual supportive care for severe COVID-19 and respiratory support with either noninvasive oxygen supplementation (n=5) or mechanical ventilation (n=19) (**Supplemental Table 1**). Patients with acute respiratory distress syndrome (ARDS) were managed with neuromuscular blockade and a protective ventilation strategy that included low tidal volume (6 mL/kg of predicted body weight) and limited driving pressure (less than 16 cmH2O) as well as optimal PEEP calculated based on the best lung compliance and PaO2/FiO2 ratio. In those with severe ARDS and PaO2/FiO2 ratio below 150 despite optimal ventilatory settings, prone position was initiated. Our

management protocol included antithrombotic prophylaxis with enoxaparin 40 to 60 mg per day. Patients did not receive routine steroids, antivirals or other anti-inflammatory or anti-platelet drugs. The SARS-CoV-2-negative control participants were not under anti-inflammatory or anti-platelet drugs for at least two weeks. All clinical information was prospectively collected using a standardized form - ISARIC/WHO Clinical Characterization Protocol for Severe Emerging Infections (CCPBR). Clinical and laboratory data were recorded on admission in all severe patients included in the study and the primary outcome analyzed was 28-day mortality (n = 11 survivors and 13 non-survivors, **Supplemental Table 2**). Age and the frequency of comorbidities were not different between severe patients requiring mechanical ventilation or noninvasive oxygen supplementation neither between survivors and non-survivors (**Supplemental Table 1 and 2**).

Statistical analysis. Statistics were performed using GraphPad Prism software version 8. All the numerical variables were tested regarding their distribution using the Shapiro-Wilk test. One-way analysis of variance (ANOVA) was used to compare differences among 3 groups following a normal (parametric) distribution, and Tukey's post-hoc test was used to locate the differences between the groups; or Friedman's test (for non-parametric data) with Dunn's post-hoc test. Comparisons between 2 groups were performed using the Student t test for parametric distributions or the Mann-Whitney U test for nonparametric distributions. Correlation coefficients were calculated using Pearson's correlation test for parametric distributions and the Spearman's correlation test for nonparametric distributions.

Study approval. Experimental procedures involving human cells from healthy donors were performed with samples obtained after written informed consent and were approved by the Institutional Review Board (IRB) of the Oswaldo Cruz Institute/Fiocruz (Rio de Janeiro, RJ, Brazil) under the number 397-07. The National Review Board approved the study protocol (CONEP 30650420.4.1001.0008) for clinical samples, and informed consent was obtained from all participants or patients' representatives.

Acknowledgments and funding

We thank the Hemotherapy Service from Hospital Clementino Fraga Filho (Federal University of Rio de Janeiro, Brazil) for providing buffy-coats. Dr. Andre Sampaio from Farmanguinhos, platform RPT11M, and Dr. Lucio Mendes Cabral from Department of Drugs and Pharmaceutics, Faculty of Pharmacy, Federal University of Rio de Janeiro (UFRJ) are acknowledged for kindly donating the Calu-3 cell. The recombinant protein Maxadilan was kindly donated to us by Dr. Ethan A. Lerner (Department of Dermatology, Massachusetts General Hospital, MA, USA). The authors are thankful to Prof. Elvira M. Saraiva (Federal University of Rio de Janeiro, Brazil) for stimulating comments and invaluable suggestions. This work was supported by Conselho Nacional de Desenvolvimento Científico e Tecnológico (CNPq), Fundação de Amparo à Pesquisa do Estado do Rio de Janeiro (FAPERJ), and by Mercosur Structural Convergence Fund (FOCEM, Mercosur, grant number 03/11). This study was financed in part by the Coordenação de Aperfeiçoamento de Pessoal de Nível Superior - Brasil (CAPES), Finance Code 001. Funding was also provided by CNPq, CAPES and FAPERJ through the National Institutes of Science and Technology Program (INCT) to

Carlos Morel (INCT-IDPN) and Wilson Savino (INCT-NIM). Thanks are due to Oswaldo Cruz Foundation/Fiocruz under the auspicious of Inova program. The funding sponsors had no role in the design of the study; in the collection, analyses, or interpretation of data; in the writing of the manuscript, and in the decision to publish the results. The authors declare no competing financial interests.

Author Contribution

Conceived the study: JRT, TMLS, DCBH; Designed the experiments: JRT, PTB, TMLS, DCBH; Performed the experiments: JRT, CQS, NFR, CRRP, CSF, SSGD, ACF, MM, VCS, LT, IGAQ, EDH, PK; Analyzed the data: JRT, PTB, IGAQ, EDH, PK, FAB, TMLS, DCBH; Wrote the paper: JRT, PTB, TMLS, DCBH. All authors reviewed and approved the manuscript.

References

1. García LF. Immune Response, Inflammation, and the Clinical Spectrum of COVID-19. Front Immunol [Internet]. 2020 Jun 16 [cited 2020 Jul 16];11. Available from: https://pubmed.ncbi.nlm.nih.gov/32612615/

2. Huang C, Wang Y, Li X, Ren L, Zhao J, Hu Y, et al. Clinical features of patients infected with 2019 novel coronavirus in Wuhan, China. Lancet [Internet]. 2020 Feb 15 [cited 2020 Jul 16];395(10223):497–506. Available from: https://isaric.tghn.org/protocols/

3. Chen G, Wu D, Guo W, Cao Y, Huang D, Wang H, et al. Clinical and immunological features of severe and moderate coronavirus disease 2019. J Clin Invest [Internet]. 2020 May 1 [cited 2020 Jul 16];130(5):2620–9. Available from: https://doi.org/10.1172/JCI137244.

4. Gupta A, Madhavan M V., Sehgal K, Nair N, Mahajan S, Sehrawat TS, et al. Extrapulmonary manifestations of COVID-19. Nat Med [Internet]. 2020 Jul 10 [cited 2020 Dec 7];26(7):1017–32. Available from: https://pubmed.ncbi.nlm.nih.gov/32651579/

5. Tang D, Comish P, Kang R. The hallmarks of COVID-19 disease [Internet]. Vol. 16, PLoS Pathogens. Public Library of Science; 2020 [cited 2020 Jul 16]. p. e1008536. Available from: https://doi.org/10.1371/journal.ppat.1008536

6. Ragab D, Salah Eldin H, Taeimah M, Khattab R, Salem R. The COVID-19 Cytokine Storm; What We Know So Far. Front Immunol [Internet]. 2020 Jun 16 [cited 2020 Jul 16];11. Available from: https://pubmed.ncbi.nlm.nih.gov/32612617/

613 7. Giamarellos-Bourboulis EJ, Netea MG, Rovina N, Akinosoglou K, Antoniadou A, Antonakos
614 N, et al. Complex Immune Dysregulation in COVID-19 Patients with Severe Respiratory
615 Failure. Cell Host Microbe. 2020 Jun 10;27(6):992-1000.e3.

616 8. Blanco-Melo D, Nilsson-Payant BE, Liu W-C, Uhl S, Hoagland D, Møller R, et al. Imbalanced
617 Host Response to SARS-CoV-2 Drives Development of COVID-19. Cell [Internet]. 2020 May
618 28 [cited 2020 Dec 7];181(5):1036-1045.e9. Available from:
619 https://pubmed.ncbi.nlm.nih.gov/32416070/

620 9. Veras FP, Pontelli MC, Silva CM, Toller-Kawahisa JE, de Lima M, Nascimento DC, et al.
621 SARS-CoV-2-triggered neutrophil extracellular traps mediate COVID-19 pathology. J Exp
622 Med [Internet]. 2020 Dec 7 [cited 2020 Dec 8];217(12). Available from:
623 https://pubmed.ncbi.nlm.nih.gov/32926098/

624 10. Radermecker C, Detrembleur N, Guiot J, Cavalier E, Henket M, d'Emal C, et al. Neutrophil
625 extracellular traps infiltrate the lung airway, interstitial, and vascular compartments in
626 severe COVID-19. J Exp Med [Internet]. 2020 Dec 7 [cited 2020 Dec 8];217(12). Available
627 from: https://pubmed.ncbi.nlm.nih.gov/32926097/

628 11. Skendros P, Mitsios A, Chrysanthopoulou A, Mastellos DC, Metallidis S, Rafailidis P, et al.
629 Complement and tissue factor–enriched neutrophil extracellular traps are key drivers in
630 COVID-19 immunothrombosis. J Clin Invest [Internet]. 2020 Nov 2 [cited 2020 Dec
631 8];130(11):6151–7. Available from: https://pubmed.ncbi.nlm.nih.gov/32759504/

632 12. Middleton EA, He XY, Denorme F, Campbell RA, Ng D, Salvatore SP, et al. Neutrophil
633 extracellular traps contribute to immunothrombosis in COVID-19 acute respiratory distress
634 syndrome. Blood [Internet]. 2020 Sep 3 [cited 2020 Dec 8];136(10):1169–79. Available
635 from: https://pubmed.ncbi.nlm.nih.gov/32597954/

636 13. Rodrigues TS, de Sá KSG, Ishimoto AY, Becerra A, Oliveira S, Almeida L, et al.
637 Inflammasomes are activated in response to SARS-CoV-2 infection and are associated with
638 COVID-19 severity in patients. J Exp Med [Internet]. 2021 Mar 1 [cited 2020 Dec 8];218(3).
639 Available from: http://www.ncbi.nlm.nih.gov/pubmed/33231615

640 14. Ferreira AC, Cardoso Soares V, de Azevedo- IG, da Silva Gomes Dias S, Fintelman-Rodrigues
641 N, Mattos M, et al. SARS-CoV-2 induces inflammasome-dependent pyroptosis and
642 downmodulation of HLA-DR in human monocytes. medRxiv [Internet]. 2020 Oct 23 [cited
643 2020 Dec 8];2020.08.25.20182055. Available from:
644 https://doi.org/10.1101/2020.08.25.20182055

645 15. Nicholls JM, Poon LLM, Lee KC, Ng WF, Lai ST, Leung CY, et al. Lung pathology of fatal
646 severe acute respiratory syndrome. Lancet [Internet]. 2003 May 24 [cited 2020 Jul
647 16];361(9371):1773–8. Available from: https://pubmed.ncbi.nlm.nih.gov/12781536/

648 16. Gu J, Gong E, Zhang B, Zheng J, Gao Z, Zhong Y, et al. Multiple organ infection and the
649 pathogenesis of SARS. J Exp Med [Internet]. 2005 Aug 1 [cited 2020 Jul 16];202(3):415–24.
650 Available from: /pmc/articles/PMC2213088/?report=abstract

651 17. Merad M, Martin JC. Pathological inflammation in patients with COVID-19: a key role for
652 monocytes and macrophages. Nat Rev Immunol [Internet]. 2020 Jun 6 [cited 2020 Dec
653 8];20(6):355–62. Available from: http://www.ncbi.nlm.nih.gov/pubmed/32488203

654 18. Schurink B, Roos E, Radonic T, Barbe E, Bouman CSC, de Boer HH, et al. Viral presence and
655 immunopathology in patients with lethal COVID-19: a prospective autopsy cohort study.

656 The Lancet Microbe [Internet]. 2020 Nov 1 [cited 2020 Dec 8];1(7):e290–9. Available from:
657 www.thelancet.com/microbe

658 19. Chiang C-C, Korinek M, Cheng W-J, Hwang T-L. Targeting Neutrophils to Treat Acute
659 Respiratory Distress Syndrome in Coronavirus Disease. Front Pharmacol [Internet]. 2020
660 Oct 9 [cited 2020 Dec 8];11:1576. Available from: www.frontiersin.org

661 20. Zhou J, Chu H, Li C, Wong BHY, Cheng ZS, Poon VKM, et al. Active replication of middle east
662 respiratory syndrome coronavirus and aberrant induction of inflammatory cytokines and
663 chemokines in human macrophages: Implications for pathogenesis. J Infect Dis [Internet].
664 2014 Sep 23 [cited 2020 Jul 16];209(9):1331–42. Available from:
665 https://europepmc.org/article/med/24065148

666 21. Tynell J, Westenius V, Rönkkö E, Munster VJ, Melén K, Österlund P, et al. Middle east
667 respiratory syndrome coronavirus shows poor replication but significant induction of
668 antiviral responses in human monocyte-derived macrophages and dendritic cells. J Gen
669 Virol [Internet]. 2016 Feb 1 [cited 2020 Jul 16];97(2):344–55. Available from:
670 /pmc/articles/PMC4804640/?report=abstract

671 22. Dickson L, Finlayson K. VPAC and PAC receptors: From ligands to function. Pharmacol Ther
672 [Internet]. 2009;121(3):294–316. Available from:
673 http://dx.doi.org/10.1016/j.pharmthera.2008.11.006

674 23. Ganea D, Delgado M. Vasoactive intestinal peptide (VIP) and pituitary adenylate cyclase-
675 activating polypeptide (PACAP) as modulators of both innate and adaptive immunity. Crit
676 Rev Oral Biol Med [Internet]. 2002;13(3):229–37. Available from: http://dx.doi.org/

677 24. Kim WK, Kan Y, Ganea D, Hart RP, Gozes I, Jonakait GM. Vasoactive intestinal peptide and
678 pituitary adenylyl cyclase-activating polypeptide inhibit tumor necrosis factor-α production
679 in injured spinal cord and in activated microglia via a cAMP-dependent pathway. J Neurosci
680 [Internet]. 2000 May 15 [cited 2020 Jul 16];20(10):3622–30. Available from:
681 https://pubmed.ncbi.nlm.nih.gov/10804204/

682 25. Larocca L, Calafat M, Roca V, Franchi AM, Leiros CP. VIP limits LPS-induced nitric oxide
683 production through IL-10 in NOD mice. Int Immunopharmacol [Internet]. 2007;7(10):1343–
684 9. Available from: http://dx.doi.org/10.1016/j.intimp.2007.05.017

685 26. Gonzalez-Rey E, Delgado M. Vasoactive intestinal peptide inhibits cycloxygenase-2
686 expression in activated macrophages, microglia, and dendritic cells. Brain Behav Immun
687 [Internet]. 2008 Jan;22(1):35–41. Available from:
688 http://dx.doi.org/10.1016/j.bbi.2007.07.004

689 27. Delgado M, Munoz-Elias EJ, Gomariz RP, Ganea D. VIP and PACAP inhibit IL-12 production
690 in LPS-stimulated macrophages. Subsequent effect on IFNγ synthesis by T cells. J
691 Neuroimmunol [Internet]. 1999 May 3 [cited 2020 Jul 16];96(2):167–81. Available from:
692 https://pubmed.ncbi.nlm.nih.gov/10337915/

693 28. Delgado M, Munoz-Elias EJ, Gomariz RP, Ganea D. Vasoactive intestinal peptide and
694 pituitary adenylate cyclase-activating polypeptide prevent inducible nitric oxide synthase
695 transcription in macrophages by inhibiting NF-kappa B and IFN regulatory factor 1
696 activation. J Immunol [Internet]. 1999 Apr 15 [cited 2020 Jul 16];162(8):4685–96. Available
697 from: http://www.ncbi.nlm.nih.gov/pubmed/10202009

698 29. Moody TW, Ito T, Osefo N, Jensen RT. VIP and PACAP: recent insights into their

699 functions/roles in physiology and disease from molecular and genetic studies. Curr Opin
700 Endocrinol Diabetes Obes [Internet]. 2011;18(1):61–7. Available from:
701 http://dx.doi.org/10.1097/MED.0b013e328342568a

702 30. Gonzalez-Rey E, Varela N, Chorny A, Delgado M. Therapeutical Approaches of Vasoactive
703 Intestinal Peptide as a Pleiotropic Immunomodulator. Curr Pharm Des [Internet]. 2007 Apr
704 1;13(11):1113–39. Available from: http://dx.doi.org/

705 31. Pozo D, Gonzalez-Rey E, Chorny A, Anderson P, Varela N, Delgado M. Tuning immune
706 tolerance with vasoactive intestinal peptide: A new therapeutic approach for immune
707 disorders. Peptides [Internet]. 2007 Sep;28(9):1833–46. Available from:
708 http://dx.doi.org/10.1016/j.peptides.2007.04.008

709 32. Temerozo JRJR, Joaquim R, Regis EGEG, Savino W, Bou-Habib DCDCDC. Macrophage
710 Resistance to HIV-1 Infection Is Enhanced by the Neuropeptides VIP and PACAP. PLoS One
711 [Internet]. 2013 Jun 20 [cited 2020 Jul 16];8(6). Available from:
712 https://pubmed.ncbi.nlm.nih.gov/23818986/

713 33. Temerozo JRJR, de Azevedo SSDDSSD, Insuela DBRDBR, Vieira RCRC, Ferreira PLCCPLC,
714 Carvalho VFVF, et al. The Neuropeptides Vasoactive Intestinal Peptide and Pituitary
715 Adenylate Cyclase-Activating Polypeptide Control HIV-1 Infection in Macrophages Through
716 Activation of Protein Kinases A and C. Front Immunol [Internet]. 2018 Jun 12 [cited 2020
717 Jul 16];9(JUN). Available from: https://pubmed.ncbi.nlm.nih.gov/29951068/

718 34. Dérand R, Montoni A, Bulteau-Pignoux L, Janet T, Moreau B, Muller JM, et al. Activation of
719 VPAC 1 receptors by VIP and PACAP-27 in human bronchial epithelial cells induces CFTR-
720 dependent chloride secretion. Br J Pharmacol [Internet]. 2004 Feb [cited 2020 Jul
721 16];141(4):698–708. Available from: /pmc/articles/PMC1574226/?report=abstract

722 35. Busto R, Prieto JC, Bodega G, Zapatero J, Carrero I. Immunohistochemical localization and
723 distribution of VIP/PACAP receptors in human lung. Peptides [Internet]. 2000 Feb [cited
724 2020 Jul 20];21(2):265–9. Available from: https://pubmed.ncbi.nlm.nih.gov/10764955/

725 36. Groneberg DA, Hartmann P, Dinh QT, Fischer A. Expression and distribution of vasoactive
726 intestinal polypeptide receptor VPAC2 mRNA in human airways. Lab Investig [Internet].
727 2001 [cited 2020 Jul 16];81(5):749–55. Available from:
728 https://pubmed.ncbi.nlm.nih.gov/11351046/

729 37. Fagerberg L, Hallstrom BM, Oksvold P, Kampf C, Djureinovic D, Odeberg J, et al. Analysis of
730 the human tissue-specific expression by genome-wide integration of transcriptomics and
731 antibody-based proteomics. Mol Cell Proteomics [Internet]. 2014 Feb [cited 2020 Jul
732 16];13(2):397–406. Available from: https://pubmed.ncbi.nlm.nih.gov/24309898/

733 38. Van Der Velden VHJ, Wierenga-Wolf AF, Adriaansen-Soeting PWC, Overbeek SE, Möller
734 GM, Hoogsteden HC, et al. Expression of aminopeptidase N and dipeptidyl peptidase IV in
735 the healthy and asthmatic bronchus. Clin Exp Allergy [Internet]. 1998 [cited 2020 Jul
736 20];28(1):110–20. Available from: https://pubmed.ncbi.nlm.nih.gov/9537773/

737 39. Dreymueller D, Uhlig S, Ludwig A. ADAM-family metalloproteinases in lung inflammation:
738 potential therapeutic targets. Am J Physiol Cell Mol Physiol [Internet]. 2015 Feb 15 [cited
739 2020 Jul 20];308(4):L325–43. Available from: https://pubmed.ncbi.nlm.nih.gov/25480335/

740 40. Bonda WLM, Iochmann S, Magnen M, Courty Y, Reverdiau P. Kallikrein-related peptidases
741 in lung diseases. Biol Chem [Internet]. 2018 Sep 25 [cited 2020 Jul 20];399(9):959–71.

742 Available from: https://pubmed.ncbi.nlm.nih.gov/29604204/

743 41. Kolb AF, Hegyi A, Maile J, Heister A, Hagemann M, Siddell SG. Molecular analysis of the
744 coronavirus-receptor function of aminopeptidase N. Adv Exp Med Biol [Internet]. 1998
745 [cited 2020 Dec 9];440:61–7. Available from: https://pubmed.ncbi.nlm.nih.gov/9782265/

746 42. Ou X, Liu Y, Lei X, Li P, Mi D, Ren L, et al. Characterization of spike glycoprotein of SARS-
747 CoV-2 on virus entry and its immune cross-reactivity with SARS-CoV. Nat Commun
748 [Internet]. 2020 Dec 27 [cited 2020 Dec 9];11(1):1620. Available from:
749 https://pubmed.ncbi.nlm.nih.gov/32221306/

750 43. Kourjian G, Xu Y, Mondesire-Crump I, Shimada M, Gourdain P, Le Gall S. Sequence-Specific
751 Alterations of Epitope Production by HIV Protease Inhibitors. J Immunol [Internet]. 2014
752 Apr 15 [cited 2020 Dec 3];192(8):3496–506. Available from:
753 http://www.jimmunol.org/content/192/8/3496

754 44. Fintelman-Rodrigues N, Sacramento CQCQ, Lima CR, da Silva FSFS, Ferreira ACAC, Mattos
755 M, et al. Atazanavir, alone or in combination with ritonavir, inhibits SARS-CoV-2 replication
756 and proinflammatory cytokine production. Antimicrob Agents Chemother [Internet]. 2020
757 Oct 1 [cited 2020 Dec 3];64(10). Available from:
758 https://pubmed.ncbi.nlm.nih.gov/32759267/

759 45. Pruijssers AJ, George AS, Schäfer A, Leist SR, Gralinksi LE, Dinnon KH, et al. Remdesivir
760 Inhibits SARS-CoV-2 in Human Lung Cells and Chimeric SARS-CoV Expressing the SARS-CoV-
761 2 RNA Polymerase in Mice. Cell Rep [Internet]. 2020 Jul 21 [cited 2020 Dec
762 3];32(3):107940. Available from:
763 https://linkinghub.elsevier.com/retrieve/pii/S2211124720309219

764 46. Delgado M, Garrido E, Martinez C, Leceta J, Gomariz RP. Vasoactive intestinal peptide and
765 pituitary adenylate cyclase-activating polypeptides (PACAP27) and PACAP38) protect
766 CD4+CD8+ thymocytes from glucocorticoid-induced apoptosis. Blood [Internet].
767 1996;87(12):5152–61. Available from: http://dx.doi.org/

768 47. Liu T, Zhang L, Joo D, Sun S-C. NF-κB signaling in inflammation. Signal Transduct Target
769 Ther [Internet]. 2017 Dec 14;2(1):17023. Available from:
770 http://www.nature.com/articles/sigtrans201723

771 48. Schomerus C, Maronde E, Laedtke E, Korf HW. Vasoactive intestinal peptide (VIP) and
772 pituitary adenylate cyclase-activating polypeptide (PACAP) induce phosphorylation of the
773 transcription factor CREB in subpopulations of rat pinealocytes: immunocytochemical and
774 immunochemical evidence. Cell Tissue Res [Internet]. 1996;286(3):305–13. Available from:
775 http://dx.doi.org/

776 49. Matt T. Transcriptional control of the inflammatory response: a role for the CREB-binding
777 protein (CBP). Acta Med Austriaca [Internet]. 2002;29(3):77–9. Available from:
778 http://dx.doi.org/

779 50. Wen AY, Sakamoto KM, Miller LS. The Role of the Transcription Factor CREB in Immune
780 Function. J Immunol [Internet]. 2010 Dec 1 [cited 2020 Dec 3];185(11):6413–9. Available
781 from:
782 http://www.jimmunol.org/content/185/11/6413http://www.jimmunol.org/content/185/1
783 1/6413.full#ref-list-1

784 51. Shenkar R, Yum H-K, Arcaroli J, Kupfner J, Abraham E. Interactions between CBP, NF-κB,

785 and CREB in the lungs after hemorrhage and endotoxemia. Am J Physiol Cell Mol Physiol
786 [Internet]. 2001 Aug 1 [cited 2020 Jul 17];281(2):L418–26. Available from:
787 https://pubmed.ncbi.nlm.nih.gov/11435217/

788 52. Toth JI, Datta S, Athanikar JN, Freedman LP, Osborne TF. Selective Coactivator Interactions
789 in Gene Activation by SREBP-1a and -1c. Mol Cell Biol [Internet]. 2004 Sep 15 [cited 2020
790 Dec 3];24(18):8288–300. Available from: /pmc/articles/PMC515064/?report=abstract

791 53. Yuan S, Chu H, Chan JF-W, Ye Z-W, Wen L, Yan B, et al. SREBP-dependent lipidomic
792 reprogramming as a broad-spectrum antiviral target. Nat Commun [Internet]. 2019 Dec 10
793 [cited 2020 Dec 3];10(1):120. Available from: https://pubmed.ncbi.nlm.nih.gov/30631056/

794 54. Cloherty APM, Olmstead AD, Ribeiro CMS, Jean F. Hijacking of Lipid Droplets by Hepatitis C,
795 Dengue and Zika Viruses—From Viral Protein Moonlighting to Extracellular Release. Int J
796 Mol Sci [Internet]. 2020 Oct 24 [cited 2020 Dec 3];21(21):7901. Available from:
797 https://pubmed.ncbi.nlm.nih.gov/33114346/

798 55. Taylor HE, Linde ME, Khatua AK, Popik W, Hildreth JEK. Sterol Regulatory Element-Binding
799 Protein 2 Couples HIV-1 Transcription to Cholesterol Homeostasis and T Cell Activation. J
800 Virol [Internet]. 2011 Aug 1 [cited 2020 Dec 3];85(15):7699–709. Available from:
801 /pmc/articles/PMC3147916/?report=abstract

802 56. Dias S da SG, Soares VC, Ferreira AC, Sacramento CQ, Fintelman-Rodrigues N, Temerozo JR,
803 et al. Lipid droplets fuel SARS-CoV-2 replication and production of inflammatory
804 mediators. Fouchier RAM, editor. PLOS Pathog [Internet]. 2020 Dec 16 [cited 2020 Dec
805 17];16(12):e1009127. Available from: https://dx.plos.org/10.1371/journal.ppat.1009127

806 57. Lee W, Ahn JH, Park HH, Kim HN, Kim H, Yoo Y, et al. COVID-19-activated SREBP2 disturbs
807 cholesterol biosynthesis and leads to cytokine storm. Signal Transduct Target Ther
808 [Internet]. 2020 Dec 1 [cited 2020 Dec 3];5(1). Available from:
809 https://pubmed.ncbi.nlm.nih.gov/32883951/

810 58. NCT0431169. Intravenous Aviptadil for Critical COVID-19 With Respiratory Failure
811 [Internet]. [ClinicalTrials.gov] Bethesda (MD): National Library of Medicine (US). [cited
812 2020 Jul 21]. Available from: https://clinicaltrials.gov/ct2/show/NCT04311697

813 59. NCT04536350. Inhaled Aviptadil for the Treatment of Moderate and Severe COVID-19
814 [Internet]. [ClinicalTrials.gov] Bethesda (MD): National Library of Medicine (US). [cited
815 2020 Jul 25]. Available from: https://clinicaltrials.gov/ct2/show/NCT04360096

816 60. Said SI. The discovery of VIP: Initially looked for in the lung, isolated from intestine, and
817 identified as a neuropeptide. Peptides [Internet]. 2007 Sep [cited 2020 Jul 20];28(9):1620–
818 1. Available from: https://pubmed.ncbi.nlm.nih.gov/17719695/

819 61. Delgado M, Munoz-Elias EJ, Martinez C, Gomariz RP, Ganea D. VIP and PACAP38 modulate
820 cytokine and nitric oxide production in peritoneal. Ann N Y Acad Sci [Internet].
821 1999;897:401–14. Available from: http://dx.doi.org/

822 62. Parry GC, Mackman N. Role of cyclic AMP response element-binding protein in cyclic AMP
823 inhibition of NF-kappaB-mediated transcription. J Immunol [Internet]. 1997 Dec 1 [cited
824 2020 Jul 16];159(11):5450–6. Available from: https://pubmed.ncbi.nlm.nih.gov/9548485/

825 63. Ollivier V, Parry GCN, Cobb RR, de Prost D, Mackman N. Elevated Cyclic AMP Inhibits NF-
826 κB-mediated Transcription in Human Monocytic Cells and Endothelial Cells. J Biol Chem
827 [Internet]. 1996 Aug 23 [cited 2020 Jul 16];271(34):20828–35. Available from:

828 https://pubmed.ncbi.nlm.nih.gov/8702838/

829 64. Luan B, Yoon YS, Lay J Le, Kaestner KH, Hedrick S, Montminy M. CREB pathway links PGE2
830 signaling with macrophage polarization. Proc Natl Acad Sci U S A [Internet]. 2015 Dec 22
831 [cited 2020 Jul 16];112(51):15642–7. Available from:
832 https://www.pnas.org/content/112/51/15642

833 65. Zhao L. Suppression of Proinflammatory Cytokines Interleukin-1 and Tumor Necrosis
834 Factor- in Astrocytes by a V1 Vasopressin Receptor Agonist: A cAMP Response Element-
835 Binding Protein-Dependent Mechanism. J Neurosci [Internet]. 2004 Mar 3 [cited 2020 Jul
836 16];24(9):2226–35. Available from: https://www.jneurosci.org/content/24/9/2226

837 66. Morris RHK, Tonks AJ, Jones KP, Ahluwalia MK, Thomas AW, Tonks A, et al. DPPC regulates
838 COX-2 expression in monocytes via phosphorylation of CREB. Biochem Biophys Res
839 Commun [Internet]. 2008 May 23 [cited 2020 Jul 17];370(1):174–8. Available from:
840 https://linkinghub.elsevier.com/retrieve/pii/S0006291X0800524X

841 67. Ernst O, Glucksam-Galnoy Y, Bhatta B, Athamna M, Ben-Dror I, Glick Y, et al. Exclusive
842 Temporal Stimulation of IL-10 Expression in LPS-Stimulated Mouse Macrophages by cAMP
843 Inducers and Type I Interferons. Front Immunol [Internet]. 2019 Aug 6 [cited 2020 Jul
844 17];10:1788. Available from:
845 https://www.frontiersin.org/article/10.3389/fimmu.2019.01788/full

846 68. Barátki BL, Huber K, Sármay G, Matkó J, Kövesdi D. Inflammatory signal induced IL-10
847 production of marginal zone B-cells depends on CREB. Immunol Lett [Internet]. 2019 Aug 1
848 [cited 2020 Jul 17];212:14–21. Available from:
849 https://linkinghub.elsevier.com/retrieve/pii/S016524781830590X

850 69. Avni D, Ernst O, Philosoph A, Zor T. Role of CREB in modulation of TNFα and IL-10
851 expression in LPS-stimulated RAW264.7 macrophages. Mol Immunol [Internet]. 2010 Apr
852 [cited 2020 Jul 17];47(7–8):1396–403. Available from:
853 https://pubmed.ncbi.nlm.nih.gov/20303596/

854 70. Park JM, Greten FR, Wong A, Westrick RJ, Arthur JSC, Otsu K, et al. Signaling Pathways and
855 Genes that Inhibit Pathogen-Induced Macrophage Apoptosis— CREB and NF-κB as Key
856 Regulators. Immunity [Internet]. 2005 Sep 1 [cited 2020 Jul 17];23(3):319–29. Available
857 from: http://www.cell.com/article/S1074761305002700/fulltext

858 71. Cheng JC, Kinjo K, Judelson DR, Chang J, Wu WS, Schmid I, et al. CREB is a critical regulator
859 of normal hematopoiesis and leukemogenesis. Blood [Internet]. 2008 Feb 1 [cited 2020 Jul
860 17];111(3):1182–92. Available from: /pmc/articles/PMC2214769/?report=abstract

861 72. Shimano H, Sato R. SREBP-regulated lipid metabolism: convergent physiology — divergent
862 pathophysiology. Nat Rev Endocrinol [Internet]. 2017 Dec 29 [cited 2020 Dec
863 3];13(12):710–30. Available from: https://pubmed.ncbi.nlm.nih.gov/28849786/

864 73. Harikumar KG, Morfis MM, Lisenbee CS, Sexton PM, Miller LJ. Constitutive formation of
865 oligomeric complexes between family B G protein-coupled vasoactive intestinal
866 polypeptide and secretin receptors. Mol Pharmacol [Internet]. 2006;69(1):363–73.
867 Available from: http://dx.doi.org/10.1124/mol.105.015776

868 74. Wu D, Lee D, Sung YK. Prospect of vasoactive intestinal peptide therapy for COPD/PAH and
869 asthma: a review. Respir Res [Internet]. 2011 Dec 1 [cited 2020 Jul 16];12(1):45. Available
870 from: https://pubmed.ncbi.nlm.nih.gov/21477377/

871 75. Onoue S, Yamada S, Yajima T. Bioactive analogues and drug delivery systems of vasoactive
872 intestinal peptide (VIP) for the treatment of asthma/COPD. Peptides [Internet]. 2007 Sep
873 [cited 2020 Jul 16];28(9):1640–50. Available from:
874 https://pubmed.ncbi.nlm.nih.gov/17537541/

875 76. Lindén A, Hansson L, Andersson A, Palmqvist M, Arvidsson P, Löfdahl CG, et al.
876 Bronchodilation by an inhaled VPAC2 receptor agonist in patients with stable asthma.
877 Thorax [Internet]. 2003 Mar 1 [cited 2020 Jul 16];58(3):217–21. Available from:
878 https://pubmed.ncbi.nlm.nih.gov/12612296/

879 77. Hamidi SA, Lin RZ, Szema AM, Lyubsky S, Jiang YP, Said SI. VIP and endothelin receptor
880 antagonist: An effective combination against experimental pulmonary arterial
881 hypertension. Respir Res [Internet]. 2011 Oct 26 [cited 2020 Jul 16];12(1). Available from:
882 https://pubmed.ncbi.nlm.nih.gov/22029879/

883 78. Hilaire RC, Murthya SN, Kadowitza PJ, Jeter JR. Role of VPAC1 and VPAC2 in VIP mediated
884 inhibition of rat pulmonary artery and aortic smooth muscle cell proliferation. Peptides
885 [Internet]. 2010 [cited 2020 Jul 16];31(8):1517–22. Available from:
886 https://pubmed.ncbi.nlm.nih.gov/20452385/

887 79. Burian B, Angela S, Nadler B, Petkov V, Block LH. Inhaled Vasoactive Intestinal Peptide (VIP)
888 improves the 6-minute walk test and quality of life in patients with COPD: The VIP/COPD-
889 trial. Chest [Internet]. 2006 Oct 1 [cited 2020 Jul 16];130(4):121S. Available from:
890 https://linkinghub.elsevier.com/retrieve/pii/S0012369216515992

891 80. Wakita A, Ohtake S, Takada S, Yagasaki F, Komatsu H, Miyazaki Y, et al. Randomized
892 comparison of fixed-schedule versus response-oriented individualized induction therapy
893 and use of ubenimex during and after consolidation therapy for elderly patients with acute
894 myeloid leukemia: the JALSG GML200 Study. Int J Hematol [Internet]. 2012 Jul 26 [cited
895 2020 Dec 9];96(1):84–93. Available from: https://pubmed.ncbi.nlm.nih.gov/22639053/

896 81. Ichinose Y, Genka K, Koike T, Kato H, Watanabe Y, Mori T, et al. Randomized double-blind
897 placebo-controlled trial of bestatin in patients with resected stage I squamous-cell lung
898 carcinoma. J Natl Cancer Inst [Internet]. 2003 Apr 16 [cited 2020 Dec 9];95(8):605–10.
899 Available from: https://pubmed.ncbi.nlm.nih.gov/12697853/

900 82. CDC. Real-time RT-PCR Primers and Probes for COVID-19 [Internet]. Centers for Disease
901 Control and Prevention. 2020 [cited 2020 Dec 4]. Available from:
902 https://www.cdc.gov/coronavirus/2019-ncov/lab/rt-pcr-panel-primer-probes.html

903 83. Wu C, Chen X, Cai Y, Xia J, Zhou X, Xu S, et al. Risk Factors Associated With Acute
904 Respiratory Distress Syndrome and Death in Patients With Coronavirus Disease 2019
905 Pneumonia in Wuhan, China. JAMA Intern Med [Internet]. 2020 Jul 1 [cited 2020 Jul
906 18];180(7):934. Available from: /pmc/articles/PMC7070509/?report=abstract

907 84. Shi S, Qin M, Shen B, Cai Y, Liu T, Yang F, et al. Association of Cardiac Injury With Mortality
908 in Hospitalized Patients With COVID-19 in Wuhan, China. JAMA Cardiol [Internet]. 2020 Jul
909 1 [cited 2020 Jul 18];5(7):802. Available from:
910 /pmc/articles/PMC7097841/?report=abstract

911 85. Guo T, Fan Y, Chen M, Wu X, Zhang L, He T, et al. Cardiovascular Implications of Fatal
912 Outcomes of Patients With Coronavirus Disease 2019 (COVID-19). JAMA Cardiol [Internet].
913 2020 Jul 1 [cited 2020 Jul 18];5(7):811. Available from:
914 https://pubmed.ncbi.nlm.nih.gov/32219356/

915

916

Figure legends

Figure 1. VIP and PACAP inhibit SARS-CoV-2 gene replication in monocytes and protect the cells from virus-mediated cytopathicity. (A, B) Monocytes were infected with SARS-CoV-2 and exposed to the indicated concentrations of (A) VIP or (B) PACAP. Virus RNA synthesis was evaluated by qPCR in the culture supernatants 24 hours after infection. (C) Cellular viability was analyzed by measuring LDH release in the supernatants of uninfected or SARS-CoV-2-infected monocytes, treated or not with VIP or PACAP. (D, E) Similar to A and B, except that cells were treated with agonists for VIP and PACAP receptors, as indicated, at different concentrations (D) or with combined equivalent doses VIP and PACAP (E). Data in A, B, D and E are shown normalized to infected cells kept only with culture medium, and in C represent means ± SD of absolute values. *$p \leq .05$; **$p \leq .01$. (A, B) n=5; (D) n=6; (D, E) n=4

Figure 2. **VIP and PACAP inhibit SARS-CoV-2 replication in Calu-3 cells, protect the cells from virus-mediated cytopathicity, and mediate transmission of viral resistance from monocytes to human lung cells.** Calu-3 cells were infected by SARS-CoV-2 and then left untreated (0) or treated with the indicated concentrations of VIP (A) or PACAP (B). After 48 hours, supernatants were collected, and viral replication was evaluated by quantifying PFUs in plaque assays. (C) Cellular viability was analyzed by measuring LDH release in the supernatants of uninfected or SARS-CoV-2-infected Calu-3 cells, treated or not with VIP (1 nM) or PACAP (50 nM). (D) Similar to A and B, except that cells were treated with agonists for VIP and PACAP receptors, as indicated, at different concentrations. (E, three bars on the left) SARS-CoV-2-infected Calu-3 cells were kept untreated (Control) or received CM (50% final dilution) from VIP- or PACAP-treated uninfected monocytes. (E, three bars on the right) SARS-CoV-2-infected Calu-3 cells were kept untreated (Control) or received CM (50% final dilution) from VIP- or PACAP-treated SARS-CoV-2-infected monocytes. After 48 hours, supernatants were collected, and viral

replication was evaluated by quantifying PFUs in plaque assay. Data are shown as means ± SD. *$p \leq .05$; **$p \leq .01$. (A, B, C, D) n=4; (E) n=5

Figure 3. **Influence of peptidases on VIP- or PACAP-induced inhibition of SARS-CoV-2 replication in pulmonary cells.** Calu-3 cells were infected with SARS-CoV-2 and treated with Bestatin at 500 nM (A), or with the indicated concentrations of VIP (B) or PACAP (C) associated or not with Bestatin 500 nM. After 48 hours, supernatants were collected, and viral replication was evaluated by quantifying PFUs in plaque assay. Data are shown as means ± SD. * and + represent $p \leq .05$ versus control (0), and # represents $p \leq .05$ of neuropeptide versus neuropeptide + Bestatin at indicated concentrations. (A, B, C) n=4

Figure 4. Association with antivirals increments the neuropeptide anti-SARS-CoV-2 effect in pulmonary cells. Calu-3 cells were infected with SARS-CoV-2 and treated with ATV 5 uM, RTV 5 uM or RDV 0.1 uM (A), or with the indicated concentrations of VIP (B) or PACAP (C) associated or not with ATV, RTV or RDV. After 48 hours, supernatants were collected, and viral replication was evaluated by quantifying PFUs in plaque assay. Data are shown as means ± SD. *, +, # and § represent $p \leq .05$ versus control (0), and "x" represents $p \leq .05$ of neuropeptide versus neuropeptide + RTV (5 nM). (A, B, C) n=4

Figure 5. **VIP and PACAP reduce production of proinflammatory mediators by SARS-CoV-2-infected monocytes and Calu-3 cells.** Monocytes and Calu-3 cells were infected with SARS-CoV-2 for 1 hour, and then exposed to VIP or PACAP (10 nM each for monocytes, 1 nM of VIP or 50 nM of PACAP for Calu-3 cells). The levels of IL-6, IL-8, TNF-α and MIF were measured in culture supernatants of monocytes after 24 hours (A), and of IL-6 and IL-8 after 48 hours for Calu-3 cells (B), by ELISA. Data represent means ± SD. *$p \leq .05$; **$p \leq .01$. (A) n=6; (B) n=4

Figure 6. **VIP and PACAP regulate the activation of transcription factors in SARS-CoV-2-infected monocytes.** Monocytes were infected by SARS-CoV-2 and, 1 hour later, the infected cells were exposed (or not - Nil) to VIP or PACAP (at 10 nM). After 24 hours, the cells were lysed and the ratios between phosphoNF-kBp65/total NF-kBp65 (A), phosphoCREB/total CREB (B), active SREBP-1/β-actin (C), and active SREBP-2/β-actin (D) were quantified by ELISA (A and B) or by western blot (C and D) in the cell lysates. Data represent means ± SD. *$p \leq .05$; **$p \leq .01$; ***$p \leq .001$. (A, B) n=3; (C, D) n=4

Figure 7. **Plasma level of VIP is elevated in patients with severe forms of COVID-19.** The levels of VIP (A) and PACAP (B) in the plasma of SARS-CoV-2-negative control participants, SARS-CoV-2-positive asymptomatic subjects, or symptomatic patients presenting mild to severe COVID-19 syndrome were quantified by ELISA. Correlation between levels of VIP and CRP (C) and levels of both neuropeptides (D) in the plasma from patients with COVID-19. Correlation between viral load and VIP (E) or PACAP (F) in mild and severe patients with detectable swabs samples. (G and I) Severe COVID-19 patients admitted to the ICU were stratified between those requiring invasive mechanical ventilation or noninvasive O_2 supplementation. (H and J) Severe COVID-19 patients were stratified according to the 28-day mortality outcome as survivors or non survivors. One outlier (CRP = 621.64 mg/dL) was excluded from the analysis in panels C-D according to the ROUT test. Linear regression (with the 95 % confidence interval) and Spearman's correlation were calculated according to the distribution of the dots (controls: grey; asymptomatics: brown; mild: green; severe: red). The horizontal lines in the box plots represent the median, the box edges represent the interquartile ranges, and the whiskers indicate the minimal and maximal value in each group. *$p \leq .05$; **$p \leq .01$.

Table 1: Characteristics of COVID-19 patients and control subjects.

Characteristics[1]	Control (n=10)	Asymptomatical/ Mild (n=6)	Severe/critical (n=24)
Age, years	53 (32 – 60)	31 (29 – 34)	58 (48 – 66)
Sex, male	4 (40%)	2 (33.3 %)	12 (50 %)
Respiratory support			
Oxygen supplementation	0 (0%)	0 (0%)	5 (20.8%)
Mechanical ventilation	0 (0%)	0 (0%)	19 (79.2%)
SAPS 3	-	-	60 (55 – 71)
PaO2/FiO2 ratio	-	-	154 (99 – 373)
Vasopressor	-	-	10 (41.6%)
Time from symptom onset to blood sample, days	-	5 (-1 – 7)[2]	14 (8 – 17)
28-day mortality	-	-	13 (54.2%)
Comorbidities			
Obesity	1 (10%)	0 (0%)	5 (20.8%)
Hypertension	1 (10%)	0 (0%)	6 (25%)
Diabetes	0 (0%)	0 (0%)	9 (37.5%)
Cancer	0 (0%)	0 (0%)	3 (12.5%)
Heart disease[3]	0 (0%)	0 (0%)	2 (8.3%)
Presenting symptoms			
Cough	0 (0%)	3 (50%)	17 (70.8%)
Fever	0 (0%)	2 (33.3%)	18 (75%)
Dyspnea	0 (0%)	0 (0%)	20 (83.3%)
Headache	0 (0%)	2 (33.3%)	3 (12.5%)
Anosmia	0 (0%)	1 (16.6%)	8 (33.3%)
Laboratory findings on admission			
Leukocytes, x 1000/µL	-	-	138 (102 – 180)
Lymphocyte, cells/µL	-	-	1,167 (645 – 1,590)
Monocytes, cells/µL	-	-	679 (509 – 847)
Platelet count, x 1000/µL	-	-	169 (137 – 218)
C Reactive Protein, mg/L[4]	0.1 (0.1 – 0.18)	0.1 (0.1 – 0.11)	178 (74 – 308)*
Fibrinogen, mg/dL[4]	281 (232 – 302)	229 (197 – 324)	528 (366 – 714)*
D-dimer, IU/mL[4]	292 (225 – 476)	191 (190 – 291)	4836 (2364 – 10816)*
IL-6, pg/mL	13 (7 – 16)	9 (7.7 – 9.2)	33.5 (19.2 – 76.7)*

[1]Numerical variables are represented as the median and the interquartile range, and qualitative variables are represented as the number and the percentage.
[2]Day of sample collection after the onset of symptoms was not computed for asymptomatic subjects.
[3]Coronary artery disease or congestive heart failure.
[4]Reference values of C reactive Protein (0.00 – 1.00), Fibrinogen (238 – 498 mg/dL) and D-dimer (0 – 500 ng/mL).
*$p < 0.05$ compared to control. The qualitative variables were compared using the two tailed Fisher exact test, and the numerical variables using the t test for parametric and the Mann Whitney U test for nonparametric distributions.

Figure 1

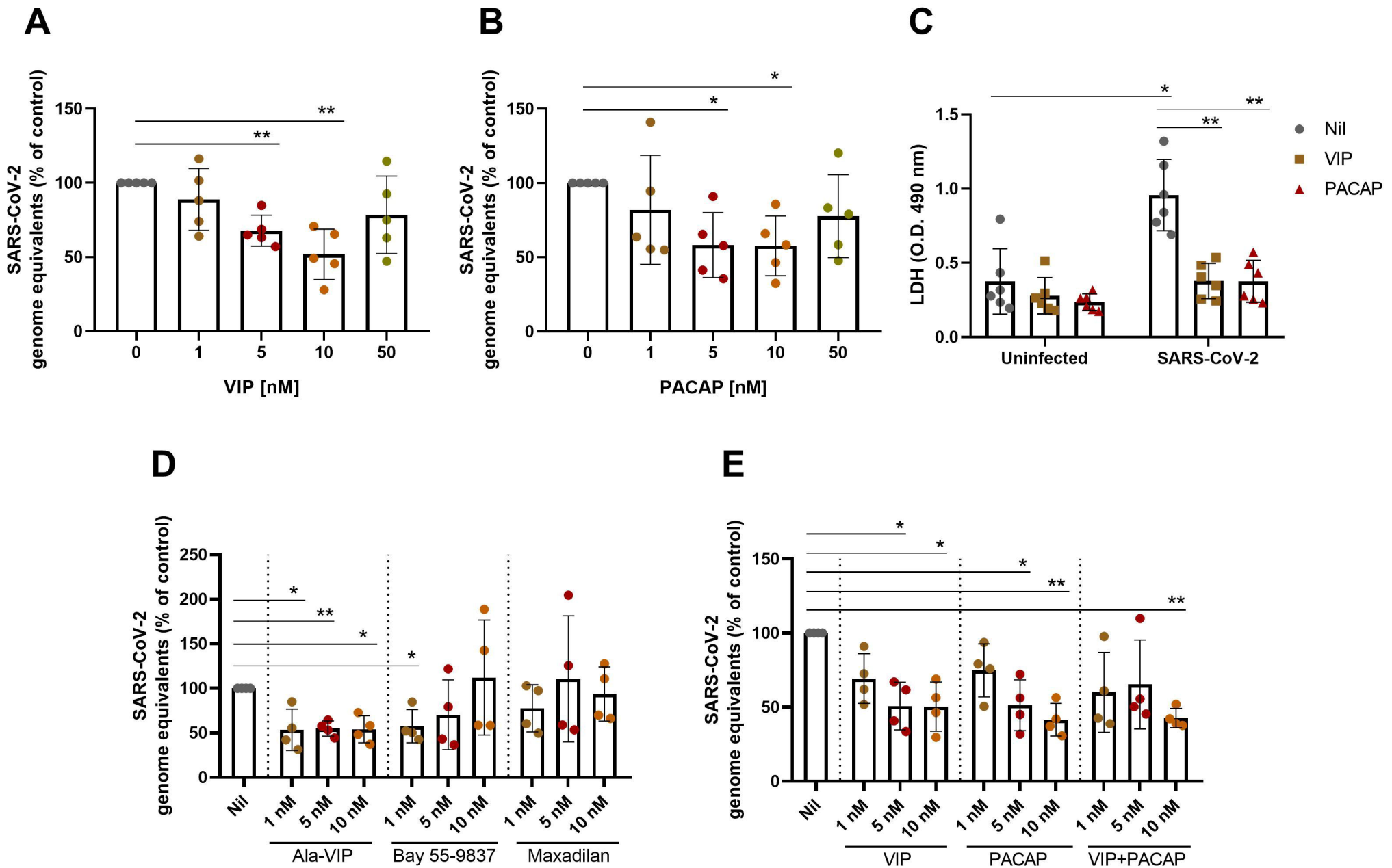
A
SARS-CoV-2 genome equivalents (% of control)
150
100
50
0
**
**
0
1
5
10
50
VIP [nM]
B
SARS-CoV-2 genome equivalents (% of control)
150
100
50
0
*
*
0
1
5
10
50
PACAP [nM]
C
LDH (O.D. 490 nm)
1.5
1.0
0.5
0.0
*
**
**
Uninfected
SARS-CoV-2
Nil
VIP
PACAP
D
SARS-CoV-2 genome equivalents (% of control)
250
200
150
100
50
0
*
**
*
*
Nil
1 nM
5 nM
10 nM
1 nM
5 nM
10 nM
1 nM
5 nM
10 nM
Ala-VIP
Bay 55-9837
Maxadilan
E
SARS-CoV-2 genome equivalents (% of control)
150
100
50
0
*
*
*
**
**
Nil
1 nM
5 nM
10 nM
1 nM
5 nM
10 nM
1 nM
5 nM
10 nM
VIP
PACAP
VIP+PACAP

Figure 2

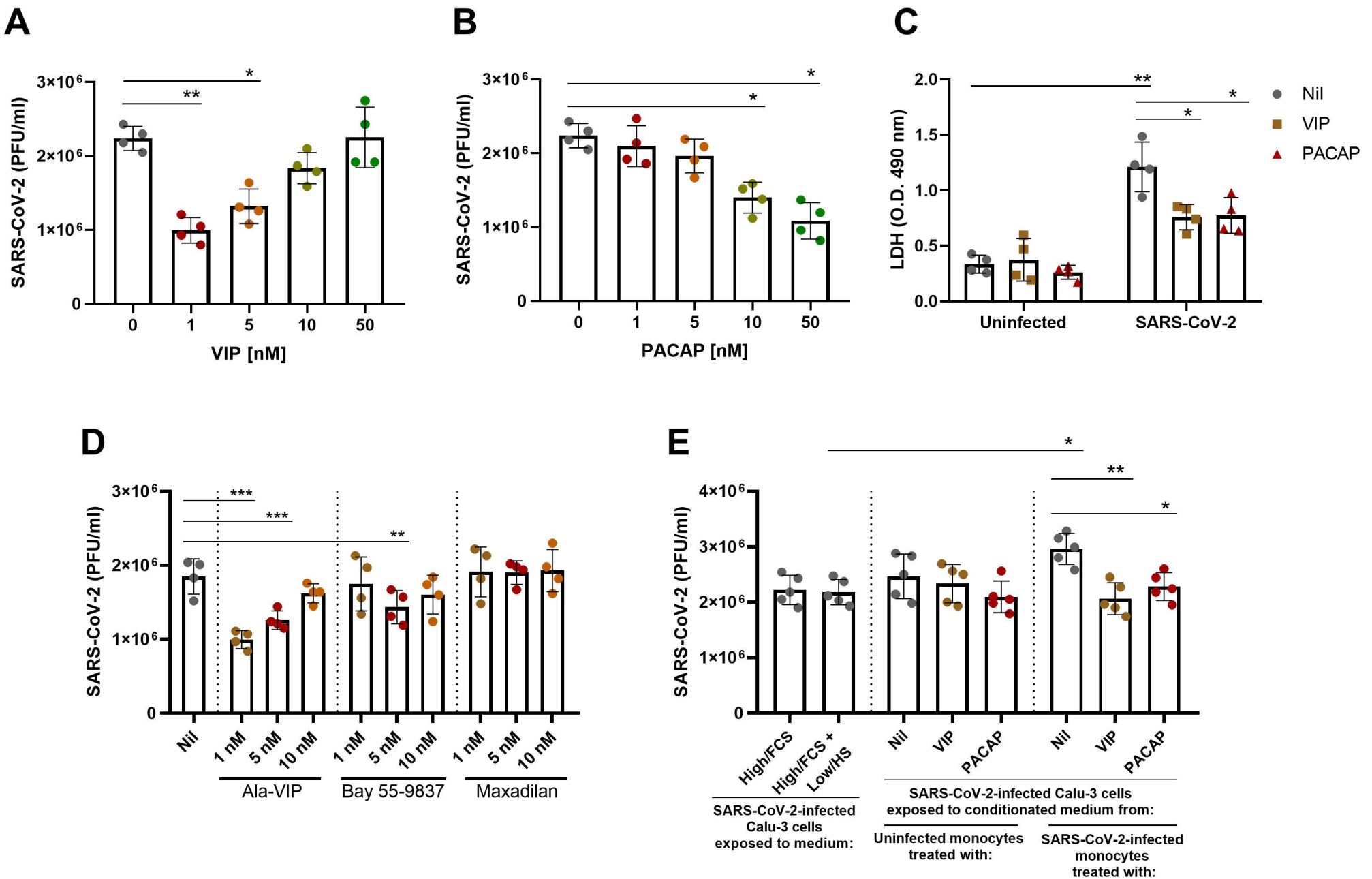
A
SARS-CoV-2 (PFU/ml)
3×10⁶
2×10⁶
1×10⁶
0
*
**
0
1
5
10
50
VIP [nM]
B
SARS-CoV-2 (PFU/ml)
3×10⁶
2×10⁶
1×10⁶
0
*
*
0
1
5
10
50
PACAP [nM]
C
LDH (O.D. 490 nm)
2.0
1.5
1.0
0.5
0.0
**
*
*
Uninfected
SARS-CoV-2
Nil
VIP
PACAP
D
SARS-CoV-2 (PFU/ml)
3×10⁶
2×10⁶
1×10⁶
0
***
***
**
Nil
1 nM
5 nM
10 nM
1 nM
5 nM
10 nM
1 nM
5 nM
10 nM
Ala-VIP
Bay 55-9837
Maxadilan
E
SARS-CoV-2 (PFU/ml)
4×10⁶
3×10⁶
2×10⁶
1×10⁶
0
*
**
*
High/FCS
High/FCS + Low/HS
Nil
VIP
PACAP
Nil
VIP
PACAP
SARS-CoV-2-infected Calu-3 cells exposed to medium:
SARS-CoV-2-infected Calu-3 cells exposed to conditionated medium from:
Uninfected monocytes treated with:
SARS-CoV-2-infected monocytes treated with:

Figure 3

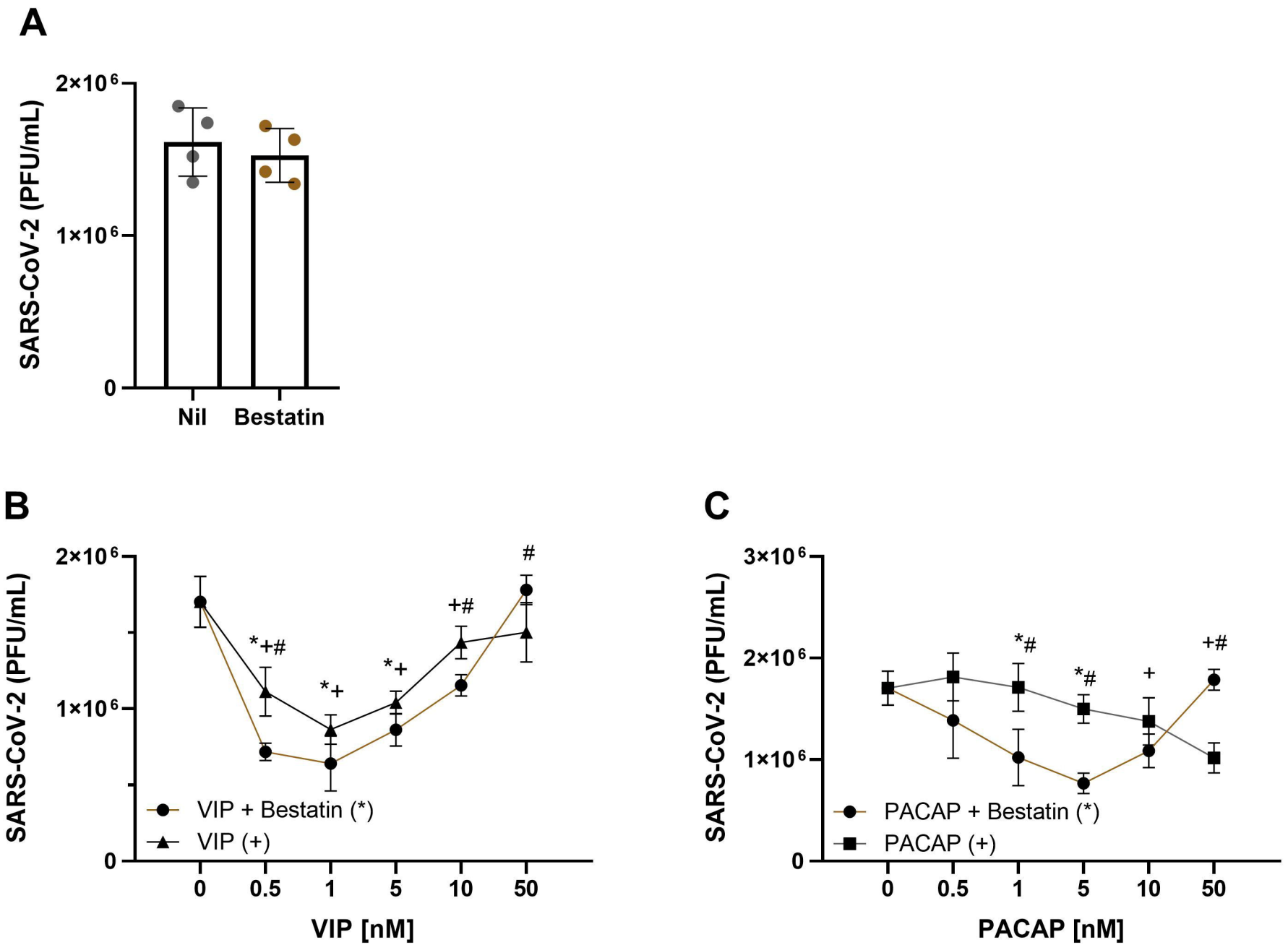
A
SARS-CoV-2 (PFU/mL)
2×10⁶
1×10⁶
0
Nil
Bestatin
B
SARS-CoV-2 (PFU/mL)
2×10⁶
1×10⁶
0
*+#
*+
*+
+#
#
VIP + Bestatin (*)
VIP (+)
0
0.5
1
5
10
50
VIP [nM]
C
SARS-CoV-2 (PFU/mL)
3×10⁶
2×10⁶
1×10⁶
0
*#
*#
+
+#
PACAP + Bestatin (*)
PACAP (+)
0
0.5
1
5
10
50
PACAP [nM]

Figure 4

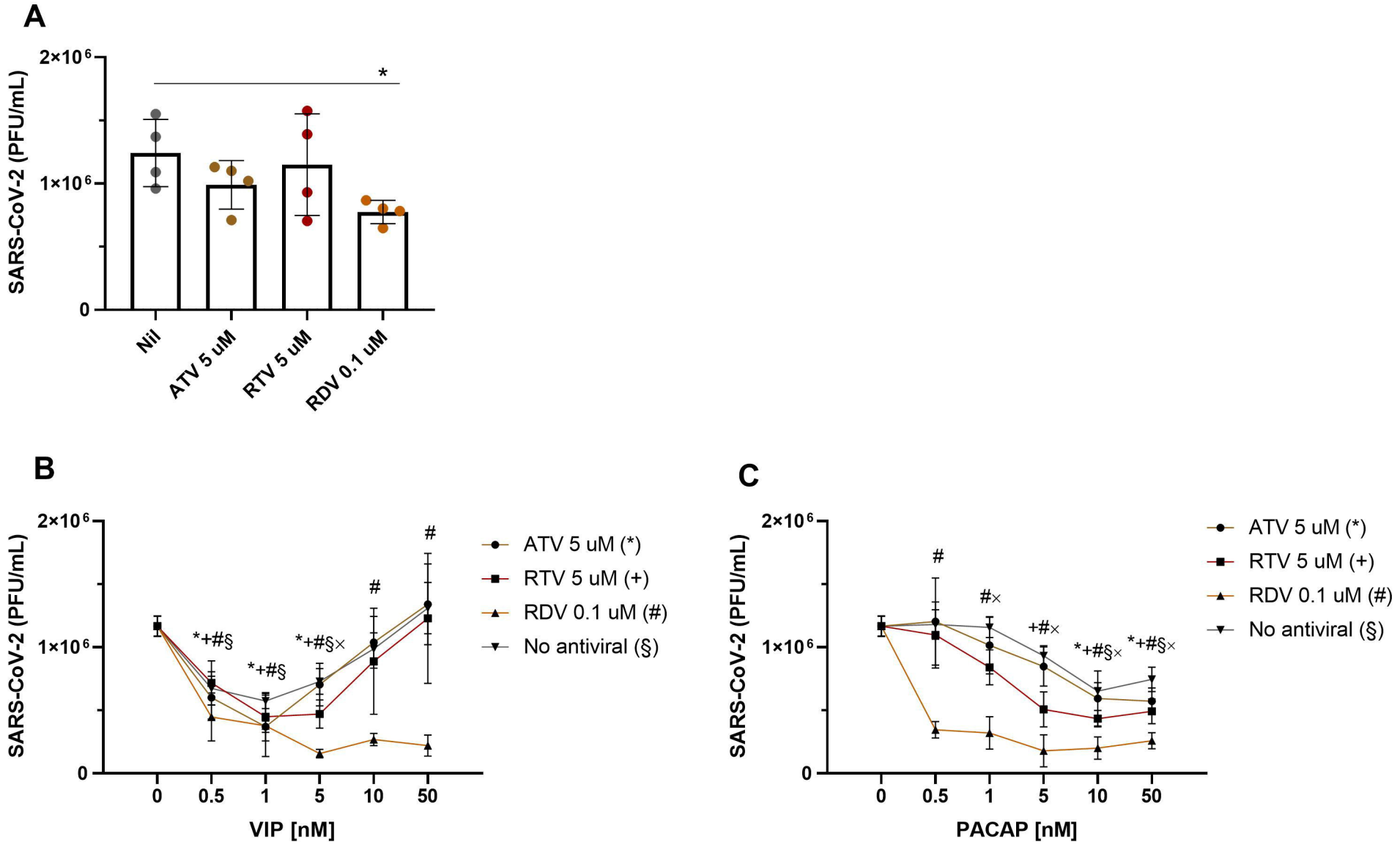
A
SARS-CoV-2 (PFU/mL)
2×10⁶
1×10⁶
0
*
Nil
ATV 5 uM
RTV 5 uM
RDV 0.1 uM
B
SARS-CoV-2 (PFU/mL)
2×10⁶
1×10⁶
0
*+#§
*+#§
*+#§×
#
#
0
0.5
1
5
10
50
VIP [nM]
ATV 5 uM (*)
RTV 5 uM (+)
RDV 0.1 uM (#)
No antiviral (§)
C
SARS-CoV-2 (PFU/mL)
2×10⁶
1×10⁶
0
#
#×
+#×
*+#§×
*+#§×
0
0.5
1
5
10
50
PACAP [nM]
ATV 5 uM (*)
RTV 5 uM (+)
RDV 0.1 uM (#)
No antiviral (§)

Figure 5

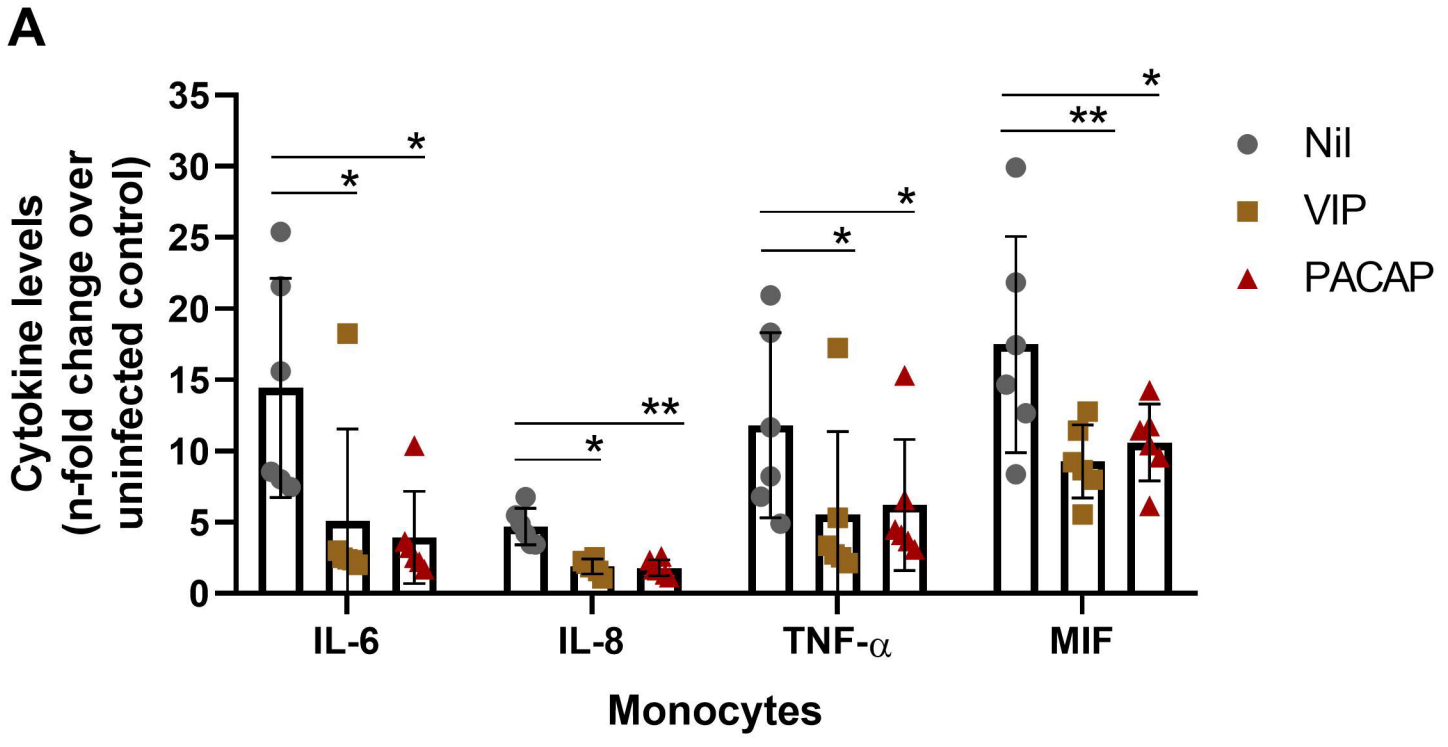
A
Cytokine levels
(n-fold change over
uninfected control)
35
30
25
20
15
10
5
0
*
*
**
*
*
*
**
*
IL-6
IL-8
TNF-α
MIF
Monocytes
Nil
VIP
PACAP

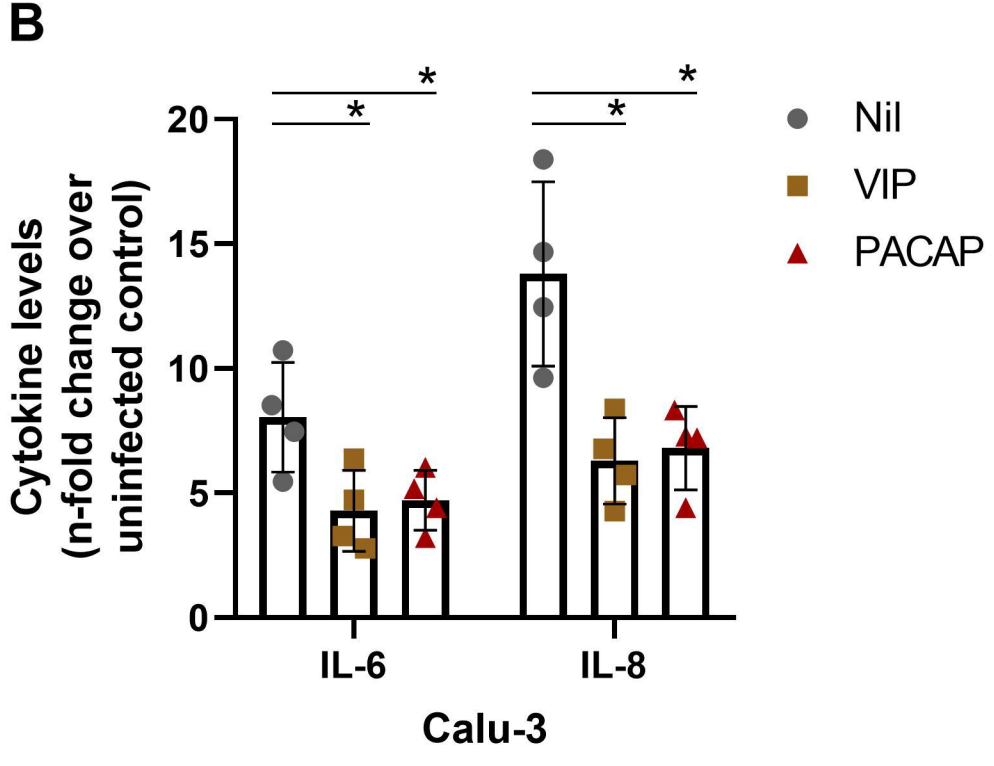
B
Cytokine levels
(n-fold change over
uninfected control)
20
15
10
5
0
*
*
*
*
IL-6
IL-8
Calu-3
Nil
VIP
PACAP

Figure 6

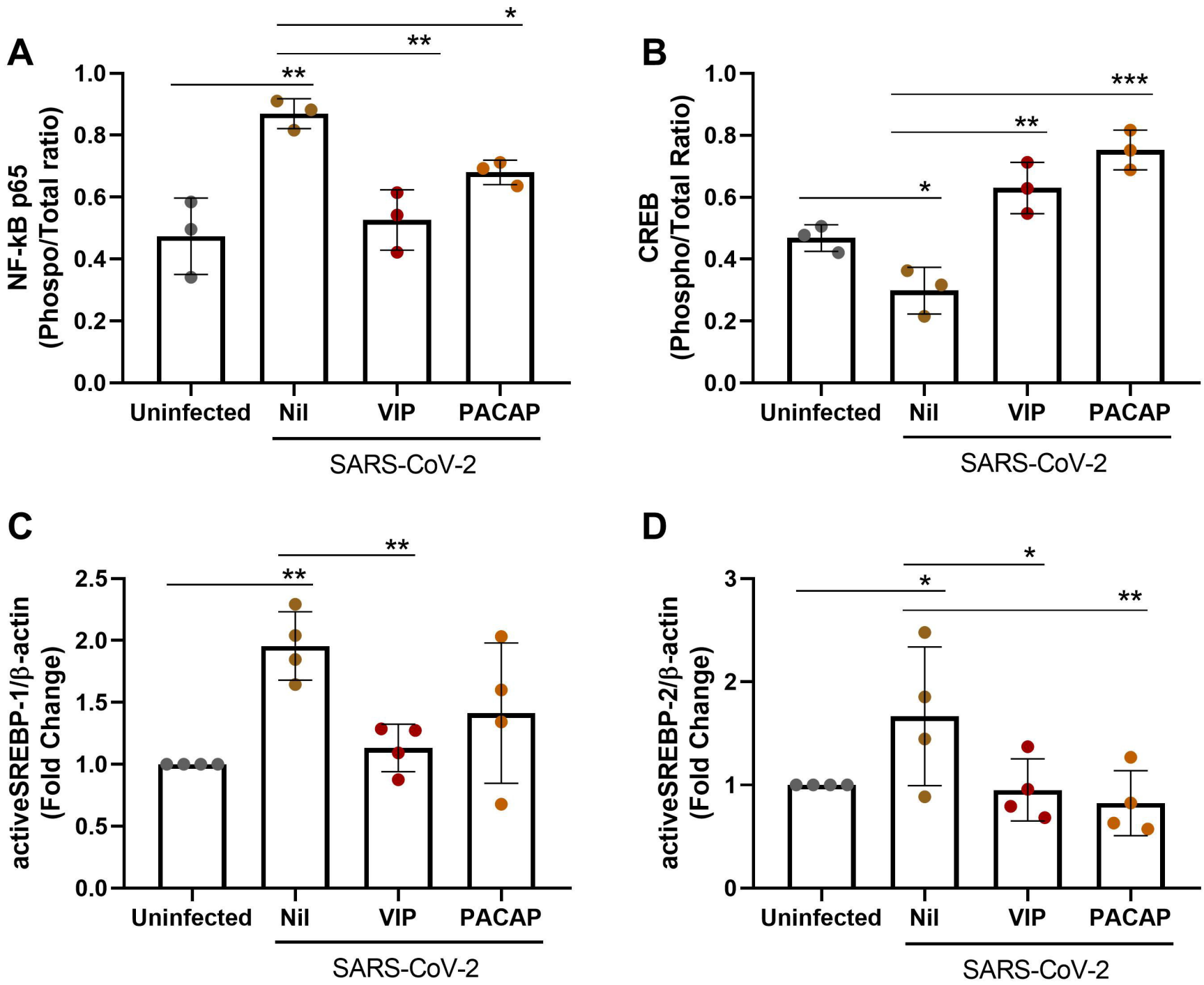
A
NF-kB p65
(Phospo/Total ratio)
1.0
0.8
0.6
0.4
0.2
0.0
**
**
*
Uninfected
Nil
VIP
PACAP
SARS-CoV-2
B
CREB
(Phospho/Total Ratio)
1.0
0.8
0.6
0.4
0.2
0.0
***
**
*
Uninfected
Nil
VIP
PACAP
SARS-CoV-2
C
activeSREBP-1/β-actin
(Fold Change)
2.5
2.0
1.5
1.0
0.5
0.0
**
**
Uninfected
Nil
VIP
PACAP
SARS-CoV-2
D
activeSREBP-2/β-actin
(Fold Change)
3
2
1
0
*
*
**
Uninfected
Nil
VIP
PACAP
SARS-CoV-2

Figure 7

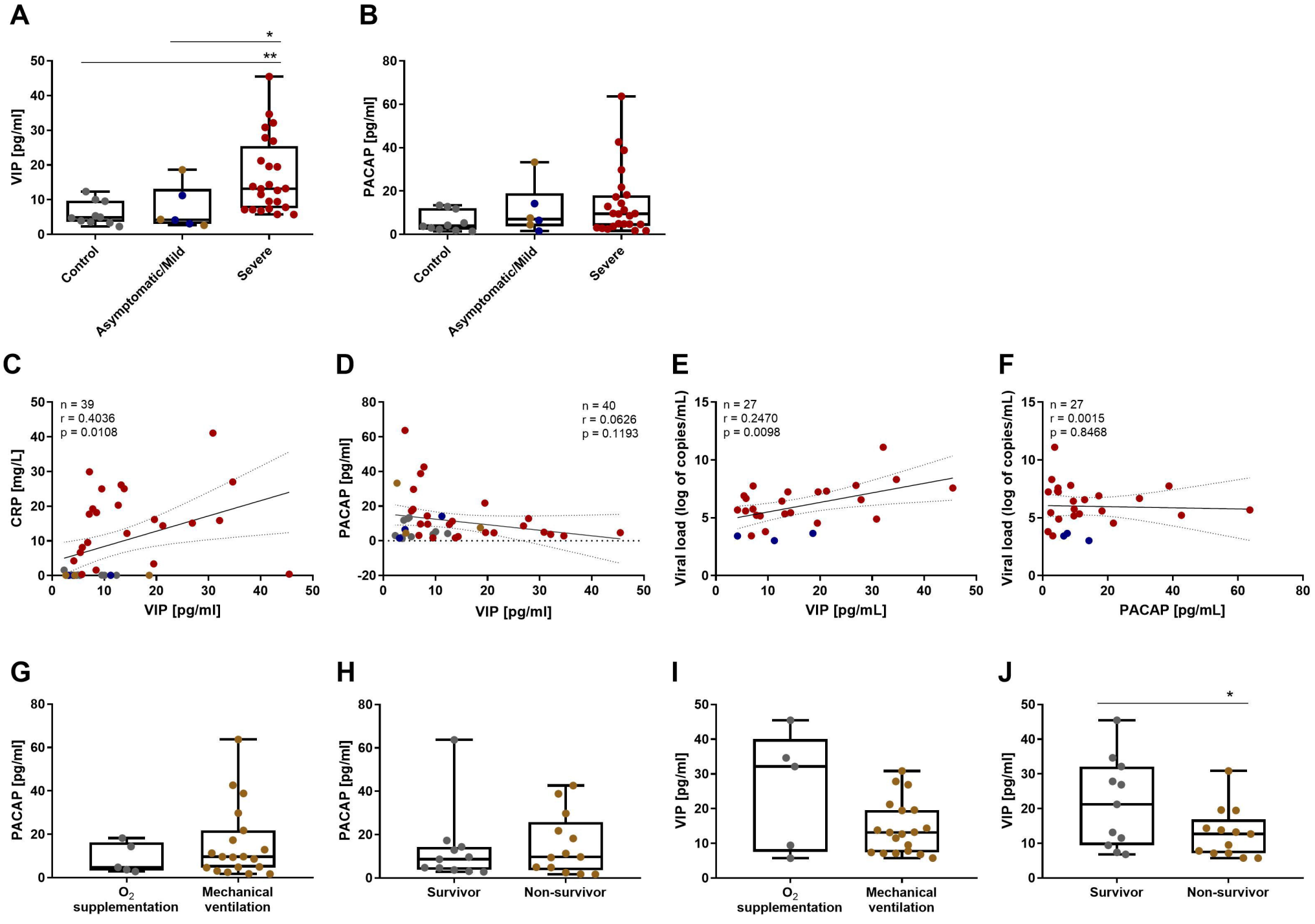
A
VIP [pg/ml]
Control
Asymptomatic/Mild
Severe
*
**
B
PACAP [pg/ml]
Control
Asymptomatic/Mild
Severe
C
n = 39
r = 0.4036
p = 0.0108
CRP [mg/L]
VIP [pg/ml]
D
n = 40
r = 0.0626
p = 0.1193
PACAP [pg/ml]
VIP [pg/ml]
E
n = 27
r = 0.2470
p = 0.0098
Viral load (log of copies/mL)
VIP [pg/mL]
F
n = 27
r = 0.0015
p = 0.8468
Viral load (log of copies/mL)
PACAP [pg/mL]
G
PACAP [pg/ml]
O2 supplementation
Mechanical ventilation
H
PACAP [pg/ml]
Survivor
Non-survivor
I
VIP [pg/ml]
O2 supplementation
Mechanical ventilation
J
*
VIP [pg/ml]
Survivor
Non-survivor